AD-A189 519 PHOTOCHEMISTRY AT STRUCTURED SURFACES: A CLASSICAL ELECTROMAGNETIC APPROA..(U) STATE UNIV OF NEW YORK AT BUFFALO DEPT OF CHEMISTRY D A JELSKI ET AL. FEB 88 1/1

UNCLASSIFIED UBUFFALO/DC/88/TR-65 N00014-86-K-0043 F/G 7/5 NL

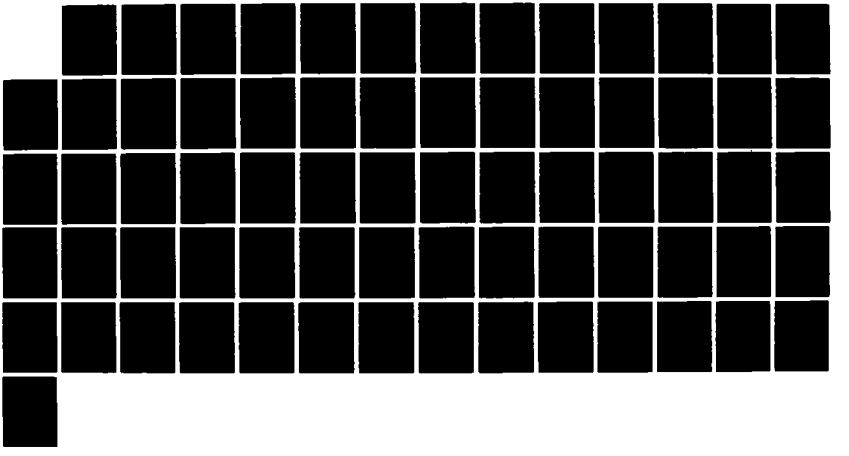

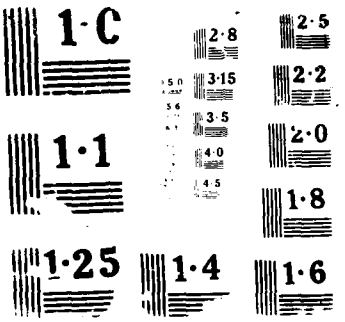
1·C
2·8
2·5
3·15
2·2
3·5
2·0
1·1
4·0
4·5
1·8
1·25
1·4
1·6

(4)

OFFICE OF NAVAL RESEARCH

Contract N00014-86-K-0043

TECHNICAL REPORT No. 65

Photochemistry at Structured Surfaces: A Classical Electromagnetic Approach

by

Daniel A. Jelski, P. T. Leung and Thomas F. George

Prepared for Publication

in

International Reviews of Physical Chemistry

Departments of Chemistry and Physics
State University of New York at Buffalo
Buffalo, New York 14260

February 1988

UNCLASSIFIED
SECURITY CLASSIFICATION OF THIS PAGE

REPORT DOCUMENTATION PAGE

Form Approved
OMB No. 0704-0188

1a. REPORT SECURITY CLASSIFICATION Unclassified	1b. RESTRICTIVE MARKINGS
2a. SECURITY CLASSIFICATION AUTHORITY	3. DISTRIBUTION / AVAILABILITY OF REPORT Approved for public release; distribution unlimited
2b. DECLASSIFICATION / DOWNGRADING SCHEDULE	
4. PERFORMING ORGANIZATION REPORT NUMBER(S) UBUFFALO/DC/88/TR-65	5. MONITORING ORGANIZATION REPORT NUMBER(S)
6a. NAME OF PERFORMING ORGANIZATION Depts. Chemistry & Physics State University of New York 6b. OFFICE SYMBOL (If applicable)	7a. NAME OF MONITORING ORGANIZATION
6c. ADDRESS (City, State, and ZIP Code) Fronczak Hall, Amherst Campus Buffalo, New York 14260	7b. ADDRESS (City, State, and ZIP Code) Chemistry Program 800 N. Quincy Street Arlington, Virginia 22217
8a. NAME OF FUNDING / SPONSORING ORGANIZATION Office of Naval Research 8b. OFFICE SYMBOL (If applicable)	9 PROCUREMENT INSTRUMENT IDENTIFICATION NUMBER Contract N00014-86-K-0043
8c. ADDRESS (City, State, and ZIP Code) Chemistry Program 800 N. Quincy Street Arlington, Virginia 22217	10. SOURCE OF FUNDING NUMBERS PROGRAM ELEMENT NO. / PROJECT NO / TASK NO / WORK UNIT ACCESSION NO

11. TITLE (Include Security Classification)

Photochemistry at Structured Surfaces: A Classical Electromagnetic Approach

12. PERSONAL AUTHOR(S)

Daniel A. Jelski, P. T. Leung and Thomas F. George

13a. TYPE OF REPORT	13b. TIME COVERED FROM ____ TO ____	14. DATE OF REPORT (Year, Month, Day)	15. PAGE COUNT
		February 1988	63

16. SUPPLEMENTARY NOTATION

Prepared for publication in International Reviews of Physical Chemistry

17. COSATI CODES			18. SUBJECT TERMS (Continue on reverse if necessary and identify by block number)	
FIELD	GROUP	SUB-GROUP	PHOTOCHEMISTRY	RAYLEIGH EXPANSION
			STRUCTURED SURFACES	PHOTODISSOCIATION
			CLASSICAL ELECTROMAGNETIC APPROACH	PERIODIC DEPOSITION

19. ABSTRACT (Continue on reverse if necessary and identify by block number)

This review article discusses several important aspects of photochemistry at structured metallic surfaces. The electromagnetic field above the surface is calculated using the Rayleigh expansion. Conditions under which this expansion is valid and simplifying approximations which make it easier to use are discussed in detail. This formalism is then applied to three different but related phenomena. First, the photodissociation rate of a molecule above a surface is calculated for laser frequencies at or near the surface plasmon resonance. It is found that there is an optimal molecule-surface distance for photodissociation. Then the absorption lineshape of a molecule is considered, where both Fano and Lorentzian lineshapes are found to be distorted as the molecule approaches the surface. Finally, laser-induced periodic deposition is discussed, and a model is developed to describe the growth rate of a cadmium grating.

20. DISTRIBUTION / AVAILABILITY OF ABSTRACT	21 ABSTRACT SECURITY CLASSIFICATION
☒ UNCLASSIFIED/UNLIMITED ☒ SAME AS RPT ☐ DTIC USERS	Unclassified
22a. NAME OF RESPONSIBLE INDIVIDUAL Dr. David L. Nelson	22b TELEPHONE (Include Area Code) (202) 696-4410 22c OFFICE SYMBOL

DD Form 1473, JUN 86 *Previous editions are obsolete*

SECURITY CLASSIFICATION OF THIS PAGE
UNCLASSIFIED

International Reviews of Physical Chemistry
in press

PHOTOCHEMISTRY AT STRUCTURED SURFACES: A CLASSICAL ELECTROMAGNETIC APPROACH

by Daniel A. Jelski, P. T. Leung and Thomas F. George

Departments of Physics & Astronomy and Chemistry
239 Fronczak Hall
State University of New York at Buffalo
Buffalo, New York 14260 USA

ABSTRACT

This review article discusses several important aspects of photochemistry at structured metallic surfaces. The electromagnetic field above the surface is calculated using the Rayleigh expansion. Conditions under which this expansion is valid and simplifying approximations which make it easier to use are discussed in detail. This formalism is then applied to three different but related phenomena. First, the photodissociation rate of a molecule above a surface is calculated for laser frequencies at or near the surface plasmon resonance. It is found that there is an optimal molecule-surface distance for photodissociation. Then the absorption lineshape of a molecule is considered, where both Fano and Lorentzian lineshapes are found to be distorted as the molecule approaches the surface. Finally, laser-induced periodic deposition is discussed, and a model is developed to describe the growth rate of a cadmium grating.

1. Introduction

Catalysis and control of chemical reactions is one of the most important tasks of a chemist. Many different methods have been tried to achieve both selectivity and high product yields. One of the best methods now available is laser chemistry, which permits the chemist a great deal of control. Laser-controlled chemical reactions have been studied for the past decade (George, 1982). A second popular method of catalyzing reactions is on surfaces, in particular metal surfaces such as platinum have long been used in organic chemistry. It is thus timely and important to inquire into the dual effects of these mechanisms combined. Hence the topic of this review article concerns the interaction of laser light with a surface, and the chemistry which can thereby be accomplished.

While more conventional laser chemistry has long been done in bulk and gas phase material, the possibility of enhancing reaction rates near a surface has been a tantalizing prospect ever since the discovery of the dramatic surface-enhanced Raman scattering (SERS) (Fleischmann et al., 1974) from pyridine adsorbed on silver electrodes. It has subsequently been learned that the most important single factor, at least for physisorbed molecules, in achieving this surface enhancement is the roughness of the substrate surface. Surface roughness couples with the radiation field to produce a plasmon along the surface, which in turn produces a large field near the surface under resonance conditions. This accounts for the SERS effect just described.

The possibility of using this enhanced surface field to effect photochemistry above and on the surface has been much studied for ten years. A review of the experimental literature was written by Goncher et al.

(1984). The present review concentrates on some theoretical aspects of the problem, and discusses some models to account for photodissociation above a surface and laser-induced deposition on a surface.

The major concern here is the application of classical electromagnetic (EM) theory to the study of possible photochemical processes occuring in the vicinity of a structured metallic surface. To this end, we and others have found the Rayleigh expansion of the surface EM fields invaluable in making the calculations both tractable and accurate. In the next section we review when and under what circustances the Rayleigh expansion is valid and shall also discuss various approximations which make practical calculations easier. In Sec. 3 we consider an application of the expansion to the calculation of the photodissociation dynamics of a molecule above a rough surface. In this case our use of the Rayleigh expansion is justified everywhere as we are considering a shallow grating. In Sec. 4 we consider the absorption lineshape of a molecule above a surface. Here we also consider the coupling between the molecule and the surface plasmon along a shallow grating. In Sec. 5 we use the Rayleigh expansion where it is exact (above the selvedge region) but also employ an approximate method of calculation valid for deeper gratings. This will permit us to discuss laser-induced chemical vapor deposition as recently observed (Brueck et al., 1982). Finally, there is a brief conclusion in Sec. 6.

2. The Rayleigh Expansion

The Rayleigh expansion has been widely used and discussed in the literature (Rayleigh, 1907; Fano, 1941; Petit, 1980). Briefly, this expansion is a solution of the homogenous Helmholtz equation

$$\Delta\vec{u} + k^2\vec{u} = 0 \quad , \tag{2.1}$$

where $\vec{u}$ represents the electric field $\vec{E}$ or the magnetic field $\vec{H}$, depending on the polarization. Maxwell's equations reduce to this simple form for time-harmonic fields in the absence of sources. Hence for light irradiating a rough surface, the Rayleigh expansion is an exact solution to Maxwell's equations outside the selvedge region. Inside the selvedge region the situation is much more complicated given the charges/currents along the surface. Then Eq. (2.1) becomes inhomogenous and other methods have to be found to solve the equation.

The Rayleigh hypothesis states that the Rayleigh expansion, exact above the selvedge region, is also a solution within the selvedge region as long as the grating is shallow. This turns out to be reasonably accurate (Glass et al., 1981) provided $\xi_1/\lambda < 0.1$, where ξ_1 is the grating amplitude (more generally, we define ξ_n as being the Fourier amplitude of the k_n wavenumber) and λ is the grating wavelength. Beyond this point the Fresnel matrix becomes ill-conditioned and hence precludes a solution of the Rayleigh equations. Agassi and George (1986a,b) have developed a means to prevent these numerical difficulties and are able to solve the Rayleigh equations for gratings of arbitrary height. They go on to maintain that this is in fact the exact solution for certain kinds of gratings, even within the

selvedge region. While we now begin to question this latter statement, we shall nevertheless find Agassi and George's dressed expansion to be very useful outside the selvedge region where its validity is guaranteed.

Let $\vec{u}$ of Eq. (2.1) refer to the electric field (p-polarization). Suppose also that we have a periodic grating with wavenumber k_g. The incident light with wavenumber $k = \omega_0/c$ is of intensity E_i. The surface lies along the $z = 0$ plane, separating two dielectrics of complex constants $\varepsilon(0)$ and $\varepsilon(1)$ above and below the surface respectively. Without loss of generality we shall henceforth assume that $\varepsilon(0) = 1$, and hence we can refer to $\varepsilon(1)$ simply as ε. Then we can write

$$\underline{E}_a = C_0(0)\vec{p}_{\alpha-}(0)\exp(i[k_0x-\alpha_0z]) + \sum_{\ell=-\infty}^{\infty} A_\ell\vec{p}_{\alpha+}(\ell)\exp(i[k_\ell x+\alpha_\ell z]) \tag{2.2}$$

$$z > \xi(x)$$

$$\underline{E}_b = \sum_{\ell} \vec{p}_{\beta+}(\ell)C_\ell\exp(i[k_\ell x-\beta_\ell z])$$

$$z < \xi(x),$$

where

$$k = \frac{\omega}{c} \qquad \varepsilon = \varepsilon_1 + i\varepsilon_2 \qquad \varepsilon_1 < -1$$

$$k_\ell = k_t + \ell k_g \qquad \alpha_\ell = (k^2 - k_\ell^2)^{1/2} \qquad \begin{matrix} \mathrm{Im}\alpha > 0 \\ \alpha_0 > 0 \end{matrix} \tag{2.3}$$

$$\beta_\ell = (\varepsilon k^2 - k_\ell{}^2)^{1/2} \qquad \mathrm{Im}\beta_\ell > 0$$

$$\vec{p}_{\alpha\pm}(\ell) = [k_\ell \hat{z} \mp \alpha_\ell \hat{x}] \qquad \vec{p}_{\beta\pm}(\ell) = \frac{1}{k}[k_\ell \underline{z} \mp \beta_\ell \underline{x}] \quad .$$

A similar pair of equations exists for the magnetic field.

$A_0(\ell)$ and $C_1(\ell)$ can be found by matching the boundary conditions. It is clear that $C_0(0)$ represents the amplitude of incoming waves and hence

$$C_0(0) = E_i \quad . \tag{2.4}$$

Toigo et al. (1977) have devised an elegant method for solving the coupled equations that result when Eq. (2.2) is matched across the boundary. The derivation is repeated in Agassi, et al. (1986a). This solution requires evaluating integrals of the following form

$$\frac{1}{\lambda}\int_0^\lambda dx\ e^{i(\alpha_n - \beta_m)\xi(x)}\ e^{-i(k_n - k_m)x} \equiv \Phi(n-m) \quad , \tag{2.5}$$

where $\xi(x)$ is the surface profile function. This integral is soluble analytically for $\xi(x)$ a sinusoidal or sawtooth function (Laks, 1981).

The solution for the sinusoidal case, where ξ_1 is the amplitude of the grating, is given by Agassi and George as

$$\sum_{\ell=-\infty}^{\infty} M_{m,\ell} A_\ell = \mu_m E_i, \tag{2.6}$$

$$\sum_{\ell=-\infty}^{\infty} N_{m,\ell} A_\ell = \nu_m E_i ,$$

where

$$M_{m,\ell} = \frac{\alpha_\ell \beta_m + k_\ell k_m}{\alpha_\ell - \beta_m} (i)^{m-\ell} J_{m-\ell}(\xi_1[\alpha_\ell - \beta_m])$$

$$N_{m,\ell} = \frac{\alpha_\ell \beta_m + k_\ell k_m}{\beta_\ell - \alpha_m} (i)^{m-\ell} J_{m-\ell}(\xi_1[\alpha_m - \beta_\ell]) \qquad (2.7)$$

$$\mu_m = \frac{-\alpha_0 \beta_m + k_0 k_m}{\alpha_0 + \beta_m} (i)^m J(\xi_1[\alpha_0 + \beta_m])$$

$$\nu_m = \frac{2\varepsilon}{\varepsilon - 1} \alpha_m \delta_{m,0} \quad .$$

The coefficients A_ℓ and C_ℓ can be determined by inverting the matrix equations (2.6).

Agassi and George have developed a scheme to assure convergence of the Rayleigh expansion under all circumstances. Toigo et al. (1977) have shown that it should be possible to do this. Agassi and George (1986) point out that

$$A_\ell e^{i\alpha_\ell \xi(x)} \to A_\ell e^{-k_g |\ell| \xi(x)} \quad \text{for } |\ell| \to \infty \quad . \qquad (2.8)$$

Now suppose that $\xi(x)$ has a large amplitude. Then when $\xi(x) << 0$ the exponential diverges, and to ensure the convergence of the total field, A_ℓ must get exponentially small. This implies that, in order to calculate the

Rayleigh coefficients, we must invert a matrix where elements $M_{m,\ell}$ are growing exponentially in size. Clearly this becomes numerically unstable. We can correct this deficiency by making the transformation

$$\tilde{A}_\ell = A_\ell e^{-i\alpha_\ell \xi_\ell} \quad \text{and} \quad \tilde{C}_\ell = C_\ell e^{-i\beta_\ell \xi_\ell} \quad . \tag{2.9}$$

We can then transform Eqs. (2.7) as

$$\tilde{M}_{\ell,m} = M_{\ell,m} e^{i\alpha_m \xi_m} \quad \text{and} \quad \tilde{N}_{\ell,m} = N_{\ell,m} e^{i\beta_m \xi_m} \quad , \tag{2.10}$$

whereby Eq. (2.6) becomes

$$\sum_{\ell=-\infty}^{\infty} \tilde{M}_{m,\ell} \tilde{A}_\ell = \mu_m E_i \tag{2.11}$$

which converges for arbitrary grating depth.

An alternative form for the Rayleigh expansion can be derived using Green's functions. The advantage here is that one also obtains a general form for the solution to the inhomogenous equation which reduces to the Rayleigh expansion outside the selvedge region, as demonstrated by Toigo et al. (1977). The form for this equation outside the selvedge region is

$$\left[\sum_{0}^{\infty} \frac{k^2 - k_\ell k_m}{\alpha_\ell} H(m) - iL(m)\right] \Phi(\ell - m) = 2\alpha_\ell E_i \delta_{\ell,0} \tag{2.12a}$$

$$\left[\sum_{0}^{\infty} \frac{\varepsilon k^2 - k_\ell k_m}{\beta_\ell} H(m) - iL(m)\right]\Phi(\ell-m) = 0 \quad . \tag{2.12b}$$

The disadvantage of this formalism is that it involves two coupled equations which are not separable in the way that equations (2.6) are. One must solve for both H(m) and L(m) simultaneously.

Recently a perturbative technique has been developed using Eq. (2.12) which permits the solution of field intensities in the shallow grating limit (Weber, 1986). The primary purpose was to calculate the dispersion relation for surface plasmons along a rough surface. Weber (1986) has extended this idea to an approximate (but quite accurate) calculation of the reflectivity. From his paper we find we can write

$$L(m) = \sum_{n} \frac{\tilde{\xi}_{n-m}}{\varepsilon\alpha_m+\beta_m}[\Lambda_{11}(m,n)L(n) + \Lambda_{12}(m,n)H(n)] - \frac{2i\alpha_0 k_z H(0)}{\varepsilon\alpha_0+\beta_0}\delta_{m,0} \tag{2.13}$$

and

$$H(m) = \sum_{n} \frac{\tilde{\xi}_{n-m}}{\varepsilon\alpha_m+\beta_m}[\Lambda_{21}(m,n)L(n) + \Lambda_{22}(m,n)H(n)] - \frac{2i\alpha_0 k_z H(0)}{\varepsilon\alpha_0+\beta_0}\delta_{m,0}, \tag{2.14}$$

where $\tilde{\xi}_{n-m}$ is a function of $\Phi(m,n)$ which reduces to the (n-m)-th Fourier component of $\xi(x)$ in the shallow grating limit. Λ_{jk} is a 2 × 2 matrix which depends only on the quantities defined in Eq. (2.3), and k_z is the perpendicular component of the incident field. As mentioned previously,

these equations are fundamentally the same as equations (2.6) above the selvedge region.

Let us now define the vector

$$\Psi_m \equiv \begin{bmatrix} L_m \\ H_m \end{bmatrix} , \tag{2.15}$$

whereby we can write Eqs. (1.14) and (1.15) as

$$\Psi_m = \phi_0 \delta_{m,0} + \sum_n \frac{V_{mn}}{\omega_m^2 - \omega^2} \Psi_n , \tag{2.16}$$

where

$$\omega_m \equiv c^2 k_m^2 \frac{\varepsilon+1}{\varepsilon}$$

and ϕ_0 is a vector containing the rightmost terms of Eqs. (2.14) and (2.15). V_{mn} is a 2 × 2 matrix which depends on Λ and also on $\tilde{\xi}_{r-m}$.

Now suppose that three modes are at or near resonance with the surface plasmon. Obviously we have to include the specular reflection as being significant since we are interested in calculating the reflectivity. Furthermore, we should include two resonant frequencies, for at least $+k_r$ and $-k_r$ will be resonant. We can then separate out these terms from Eq. (2.16) to yield

$$\Psi_m = \phi_0 \delta_{m,0} + \sum_{n=0,m_1,m_2} \frac{V_{mn}}{\omega_m^2 - \omega^2} \Psi_n + \sum_{n\neq 0,m_1,m_2} \frac{V_{mn}}{\omega_m^2 - \omega^2} \Psi_n . \tag{2.17}$$

For non-resonant terms ($n \neq 0, m_1, m_2$) we can make the approximation

$$\Psi_p = \sum_{n=0,m_1,m_2} \frac{V_{pn}}{\omega_p^2 - \omega^2} \Psi_n, \qquad p \neq 0,\ m_1,\ m_2 \quad . \tag{2.18}$$

Substituting this back into Eq. (2.17) and doing some algebra, we get

$$\Psi_m = \phi_0 \delta_{m,0} + \sum_{n=0,m_1,m_2} [V_{mn} + \sum_{p\neq 0,m_1,m_2} \frac{V_{mp} V_{pn}}{\omega_p^2 - \omega^2}] \Psi_n (\omega_m^2 - \omega^2)^{-1/2}. \tag{2.19}$$

Recalling that V_{mp} is a 2×2 matrix, we are led to a 6×6 matrix equation for Ψ_m. However, for modes that are resonant we can use the relation

$$L(n) = \frac{\beta_n}{\epsilon} H(n) \quad \text{for } n = 0,\ m_1,\ m_2 \quad . \tag{2.20}$$

Then the system reduces to a 3×3 matrix which can be solved analytically.

Weber numerically tested this method against the exact theory. His model was a silver surface with a sawtooth grating profile, $\lambda = 8000$ Å. The incident frequency was varied between about 2.15 and 2.25 eV, with the "plasmon dip" in the reflectivity observed at about 2.21 eV (see Fig. 1). For a grating height of 300 Å the approximate method corresponds almost exactly to the exact calculation. For $\xi_1 = 600$ Å some error is introduced but the method still works remarkably well. The result as a function of grating height is shown in Table 1.

Our group has found an even simpler method for calculating the plasmon field intensity at resonance (Jelski et al., 1987). Rather than use the extinction theorem results of Eq. (2.12) as Weber did, we instead use the Rayleigh-Fano expansion of Eq. (2.2). This implies that we need not introduce the vector Ψ_n as Weber does, but since the equations are separable we obtain a scalar equation. However, since we restrict ourselves to the resonance frequency, we can further simplify the problem by neglecting specular reflection. Hence our method will not yield accurate values for the reflectivity away from resonance. We have developed it to calculate the plasmon intensity as a function of grating height. In this application it appears quite suitable (see Fig. 2), and the results compare favorably with those of Weber. We shall investigate the application more in Sec. 5. Unlike Weber, our formalism is applied to a sinusoidal surface, and hence we can use the results embodied in Eqs. (2.6) and (2.7).

We begin with Eqs. (2.6). Let us assume for specificity that A_1 is resonant, and hence

$$A_1 >> A_m \qquad m \neq 1. \tag{2.21}$$

Then we can rewrite Eqs. (2.6) as

$$M_{11}A_1 + \sum_{m\neq 1} M_{1,m}A_m = \mu_1 E_i \tag{2.22}$$

or

$$A_1 = \frac{\mu_1 E_i + \sum_{m\neq 1} M_{1m} A_m}{M_{11}}. \tag{2.23}$$

The similarity in spirit to Weber's derivation should now be obvious. Continuing in that vein, we approximate A_m as

$$A_m = \frac{\mu_m E_i - M_{m,1} A_1}{M_{mm}} \quad , \tag{2.24}$$

and substituting this into Eq. (2.23), we obtain

$$A_1 \cong \frac{(\mu_1 - \sum_{p\neq 1} \frac{M_{1p}}{M_{pp}} \mu_p) E_i}{M_{11} - \sum_{p\neq 1} \frac{M_{1p} M_{p1}}{M_{pp}}}. \tag{2.24}$$

For normal incidence, however, it is not possible to ignore the A_{-1} term since, by symmetry, $A_1 = A_{-1}$. Including this effect we get

$$A_1 \cong \frac{(\mu_1 - \sum_{p\neq 1} (M_{1p} + M_{1-p}) \frac{\mu_p}{M_{pp}}) E_i}{[(M_{11} + M_{1-1}) - \sum_{p\neq 1} (M_{1p} + M_{1-p})(M_{p1} + M_{p-1}) \frac{1}{M_{pp}}}} \quad . \tag{2.26}$$

To ensure convergence we can use the dressed form of these equations as previously discussed.

The results of this method are shown in Fig. 2. We see that the approximate method overstates the exact result, but that it is

qualitatievely correct. On comparison with Weber's data (Table I), we find the same qualitative behavior despite the differences in the model studied. How does our method compare with that of Weber? The first obvious fact is that we have neglected the specular reflection from our calculation. Hence our calculation of the reflectivity is obviously not possible. However, at plasmon resonance the reflection may be considered small and hence neglected. Thus our method is thus suitable for calculating resonance plasmon field intensities. Weber has also included two other resonant frequencies, m_1 and m_2. We have done the same for the case of normal incidence. For other cases it would seem unlikely that there would be two resonant frequencies very close together. Hence the restriction of normal incidence is probably not severe from the standpoint of practical application. In conclusion, we note that while Weber's method is more general, ours is easier to use and it seems that the derivation is more transparent. Further, under conditions where our method applies it appears to be just as accurate.

We continue our discussion of the Rayleigh expansion by considering an important special case, namely the shallow grating limit. In this case $\Phi(n-m)$ can be expanded to first order in $\xi(x)$. This has been discussed in an excellent review by Maradudin (1982), and it is also the approach taken by Jha et al. (1980). We shall use these results in Sec. 3. To first order in $\xi(x)$, we have

$$\Phi(n-m) \approx \delta_{n-m} + i(\alpha_n - \beta_m)\xi_{n-m} \quad . \tag{2.27}$$

In this case, Eqs. (2.7) simplify to

$$M_{m,\ell} = i^{m-\ell}(\alpha_n\beta_m + k_\ell k_m)\xi_{n-m} \quad , \qquad m \neq \ell$$

$$M_{m,m} = \frac{\alpha_m\beta_m + k_m^2}{\alpha_m - \beta_m} \tag{2.28}$$

$$\mu_m = i^m(-\alpha_0\beta_m + k_0 k_m)\xi_m \quad .$$

If we insert these results into Eq. (2.26), we get the first-order approximation for the plasmon field intensity. The result (with different notation) is given in the next section by Eqs. (3.6) and (3.7) and will be discussed further in Sec. 5. Similarly, by setting

$$M_{11} = 0 \quad , \tag{2.29}$$

one recovers the flat surface dispersion relation. For real ε this is given by Eq. (3.8). The case of complex ε will be discussed in Sec. 5.

We close by considering some attempts to solve the inhomogenous equation valid in the selvedge region. This has been done analytically for the case of the square well grating (Sheng et al., 1982). The result has been extended (Lee et al., 1985) by taking advantage of the scheme depicted in Fig. 3. It is possible to determine the field strength at each layer (exactly) from the result for the previous layer. A recursion relation thus develops which gives the total field everywhere exactly.

3. Photodissociation

While both vibrational and electronic molecular spectroscopy on rough metallic surfaces have been studied extensively (Avouris et al., 1984;

Moskovits, 1985), the general area of photochemistry at such surfaces has also attracted much activity in recent years (Goncher et al., 1984). In particular, the process of photodissociation of gas molecules at such surfaces is of great interest since it is the first step that one must study in order to understand and control the various phenomena ranging from the deposition of molecules (Brueck et al., 1982) (see Sec. 4) to laser-induced heterogeneous catalysis (Lin et al., 1984). In this section, we shall explore briefly both experimental and theoretical work done in recent years in this area. We shall emphasize the roughness and surface plasmon excitations of metallic surfaces, in constrast to some previous reviews on spectroscopy where other excitations such as electron-hole pairs and phonons have been stressed, in which cases the role of the surface roughness has been minor (Avouris et al., 1984). Furthermore, we shall limit ourselves mainly to physisorbed molecules where bonding between the admolecule and the surface can be neglected. For the case of chemisorbed molecules due to charge-transfer processes occurring between the admolecule and the surface (Lundqvist, 1984), the problem has become more complicated, since under these circumstances photodesorption will accompany photodissociation of the admolecules as a competing process, which requires a more difficult theoretical analysis. Nevertheless, experimental work has been done along these lines (Bourdon et al., 1984, 1986).

We begin by reviewing some experiments recently done on the photofragmentation of physisorbed molecules on rough metallic surfaces. The first one we would like to mention is that carried out at Lincoln Laboratory (Ehrlich et al., 1981) in which metal-alkyl compounds are deposited on a host substrate with both gas and liquid adlayers coexisting on the

substrate. Photodissociation of such absorbates is studied by using a UV laser of weak intensity (~3 mW) at 257.2 nm and for two different metal alkyls, dimethyl cadmium, $Cd(CH_3)_2$, and hexamethyl alminium, $Al_2(CH_3)_6$. It is found that for the case of $Cd(CH_3)_2$, most of the dissociation occurs in the gas phase well above the substrate, and for the case of $Al_2(CH_3)_6$ most of the dissociation occurs well into the adlayers. This seems to imply an optimal molecule-surface distance at which maximum dissociation occurs. Indeed, in performing an experiment of photodecomposition of pyridine molecules adsorbed on roughened silver Ag(110) surface at 406.7 nm laser frequency, a group at Berkeley (Goncher et al., 1984) has observed the existence of such an optimal distance. The next experiment we want to mention is that carried out by the Exxon group (Garoff et al., 1982), where photodegradation of dye molecules (rhodamine 6G) by a visible laser of ~0.1 W/cm^2 has been carried out on top of a silver-island film on a silica substrate. Enhanced photodegradation is hardly observed in this experiment, but rather for molecules close to the silver islands, decreased fragmentation rate is seen. On the other hand, an experiment conducted by Columbia researchers has reported the observation of enhanced photodissociation of organometallic molecules at metallic island surfaces (Chen et al., 1983). In this experiment, the same UV (257.2 nm) laser (Ehrlich et al., 1981) is used to dissociate $Cd(CH_3)_2$ on top of a dielectric substrate which is covered by a mixture of spherical cadmium and gold pellets. These spheres are observed to grow to ellipsoids due to subsequent deposition of the Cd molecules following the dissociation process. Enhanced growth rate has been observed for Cd spheres but not for Au spheres. As we shall see below, these seemingly contradictory observations (Garoff et al.,

1982; Chen et al., 1983) can be explained by introducing the concept of a critical molecule-surface distance into the description of the dissociation phenomena. Let us first review briefly some theoretical work which helps serve as a basis for such a concept.

Ever since the first observation of surface-enhanced Raman scattering (SERS) (Fleischman et al., 1974), a large amount of effort has been devoted to the theoretical explanation of this phenomenon and the investigation of the possible surface enhancement of other photochemical processes (Chang et al., 1982; Moskovits, 1985). To this latter effort, we want to mention in particular the work by Nitzan et al. (1981), Weitz et al. (1983) and Gersten et al. (1985), who have studied both resonant and non-resonant processes including Raman, resonance Raman, fluorescence and photoabsorption phenomena. In most of these cases, the four-level model has been found to be quite successful in the explanation of these various phenomena (Weitz et al., 1983). The main physical mechanisms have been identified to include the image effect, the shape (lightening rod) effect and the surface plasmon (SP) effect. While the first one is found to be very small in ordinary SERS, the last one is viewed as the main mechanism leading to such dramatic enhancement. This is true at least for physisorbed molecules in which the bonding effect between the admolecule and surface can be neglected, though the situation may be different for chemisorbed molecules (McCall et al., 1980). Two conditions must be met in order for the plasmon enhancement effect to be plausible , namely, the metallic surface must be rough and the incident light frequency should satisfy the SP resonance condition. Roughness implies the excitability of SP, and the resonance condition ensures a large magnitude of the SP field which then leads to strong

absorption by the molecular system on top of the surface. These investigators have modelled the surface roughness as a collection of very tiny spheres and have provided specific details for an isolated sphere and the case with two neighboring spheres (Gersten et al., 1985). Furthermore, they have extended their investigation to the possibility of surface-enhanced photodissociation for the case of direct (fast) dissociation. This latter process can be treated on the same footing as the absorption process since the dissociation takes place on a time scale of the order of 10^{-14} s following absorption, leading to a yield of almost unity for such reactive processes (Nitzan et al., 1981). To calculate this absorption/dissociation cross section, the classical approach has been taken in which the molecule is modelled as a point dipole ($\vec{\mu}$) satisfying the damped oscillator equation

$$\ddot{\vec{\mu}}(t) + (\omega_M^0)^2\,\vec{\mu}(t) + \gamma_M^0\,\dot{\vec{\mu}}(t) = (\omega_M^0)^2\,\alpha_M\vec{E}(\omega,t) \quad , \tag{3.1}$$

where ω_M^0 and γ_M^0 are, respectively, the molecular frequency and decay rate in the absence of the surface, α_M is the molecular polarizability, and $\vec{E}(\omega,t) = \vec{E}(\omega)e^{-i\omega t}$ is the external field at the site of the molecule. Let us write this field in the form

$$\vec{E}(\omega) = \vec{E}_0 + \vec{E}_r + \vec{E}_{sp} + \vec{E}_{im} = [1 + A(\omega)]\cdot\vec{E}_0(\omega) + G(\omega)\cdot\vec{\mu}(\omega) \quad , \tag{3.2}$$

where each term stands for the incident, reflected, surface plasmon and image fields, respectively, and the coefficients $A(\omega)$ and $G(\omega)$ are in general tensors. A Fourier analysis of Eq.(3.1) then admits the solution

$$\mu(\omega) = \frac{\alpha_M(\omega_M^0)^2}{\omega_M^2-\omega^2-i\omega\gamma_M}\,\hat{n}_\mu\cdot[1+A]\cdot\vec{\varepsilon}_0 \quad , \tag{3.3}$$

where $\hat{n}_\mu$ is the unit vector of the direction of the molecular dipole and we have assumed $\vec{E}_0 = \vec{\varepsilon}_0\, e^{-i\omega t}$. Note that ω_M and γ_M are, respectively, the "surface-modified" frequency and decay rate which are to be determined by the image field $G(\omega)\cdot\vec{\mu}(\omega)$ in Eq.(3.2) (Gersten et al., 1985). Using Eq.(3.3), the Poynting flux absorbed by the molecular system has been calculated (Gersten et al., 1985), and together with the result for the incident flux this leads to the absorption cross section

$$\sigma(\omega) = 2\pi c\alpha^2 a_0 |\hat{n}_\mu\cdot[1+A]\cdot\hat{n}_0|^2\,\frac{\gamma_M}{(\omega-\omega_M)^2-(\frac{\gamma_M}{2})^2} \quad , \tag{3.4}$$

where $\hat{n}_0 = \vec{\varepsilon}_0/\varepsilon_0$, α is the fine structure constant and a_0 the Bohr radius. It is clear from Eq. (3.4) that $\sigma(\omega)$ exhibits the general Lorentzian structure and that surface effects enter into the absorption/dissociation process via the terms $A(\omega)$, ω_M and γ_M . Since under most circumstances the change of the molecular frequency due to the presence of the image field is almost completely negligible (Chance et al., 1978), we shall assume $\omega_M \cong \omega_M^0$ in most of our discussion below. It then becomes clear from Eq.(3.4) that two competing mechanisms exist for such processes due to the presence of the surface, namely, the enhanced local field ($A(\omega)$), which tends to increase the rate of absorption/dissociation processes, and the increased decay rate (γ_M), which tends to suppress such processes (Garoff et al., 1982; Gersten et al., 1985). Because of this, the molecule-surface separation dependence

(d) for this kind of processes is very different from that for ordinary SERS (Murray, 1982). For the latter where only the enhanced SP field plays an important role, the enhanced SERS cross section is expected to decrease monotonically as d increases. Because of this difference in distance dependence, we shall see that the concepts of the critical and optimal distance mentioned above should be introduced into the description of the photodissociation process. Before we present the results from model calculations, however, we shall summarize some work dealing with the quantities $A(\omega)$ and $\gamma_M(\omega)$.

The problem of surface electromagnetic (EM) fields has attracted much attention in the past two decades. A large number of investigations have been made in order to determine the extent to which the classical macroscopic Maxwell theory may be applicable. This covers the cases for different polarizations (s/p) of the incident light, different kinds of dielectric (metallic/nonmetallic) surfaces and different surface morphologies (flat/rough). We refer to the recent comprehensive review article on this subject by Feibelman (1982), particularly his detailed discussion on the nonlocal EM theory for the description of surface optics. Here we shall only outline briefly the case for a rough metallic surface, with special attention given to the surface plasmon mode.

Theoretical modelling of surface roughness falls into the following three catagories:

(i) Periodic roughness: This class of regular roughness is normally represented by a grating. For the case of a shallow sinusoidal grating, the surface fields have been calculated using the Rayleigh method and a phenomenological approach (Marvin et al., 1975;

Maradudin et al., 1975; Equiluz et al., 1983; Maradudin, 1982). The case for a deep grating ($\xi/\lambda_g \gtrsim 0.072$) has also been treated using the extinction theorem (Toigo et al., 1977) and the dressed Rayleigh expansion approach (Agassi et al., 1986).

(ii) Random roughness: This kind of surface is specified by a spatial correlation function $\langle\zeta(\vec{r}-\vec{r}')\rangle$, where very often a Gaussian distribution of roughness is assumed so that $\langle\zeta(\vec{r}-\vec{r}')\rangle \sim \exp(|\vec{r}-\vec{r}'|^2/a^2)$ with both coordinates $\vec{r}$ and $\vec{r}'$ lying on the surface. The surface EM fields for this case have been treated using a Green function approach, mainly by the Irvine group (Maradudin et al., 1975; Equiluz et al., 1983 Maradudin, 1982).

(iii) Island surfaces: This kind of surface is usually modelled as a collection of spheroids which can be spheres or ellipsoids, eitherregularly (periodically) or randomly distributed. Normally the case for one spheroid is worked out, and the final result is then obtained by the principle of superposition of the contributions from the other spheroids. The surface EM fields for this case haveattracted great interest recently (Meier et al., 1985; Cline et al., 1986).

As for our application here to the dissociation process described by Eq.(3.4), we shall assume the simplest geometry to illustrate the ideas of the various competing mechanisms and the various distance concepts. Specifically, we shall consider the rough surface as a shallow sinusoidal grating (see Fig. 4). As mentioned above, the surface EM fields have been worked out by a phenomenological approach with the application of the Rayleigh hypothesis (Marvin et al., 1975; Jha et al., 1980). Assuming a

notation of $\vec{E} = \begin{pmatrix} E_{\parallel} \\ E_z \end{pmatrix}$ with $E_{\parallel}$ being the component on the xy-plane (i.e., along the surface) and E_z the z-component, the field-amplification factor $A(\omega)$ for p-polarized incident laser light can be written as (Leung et al., 1986)

$$A(\omega) = \begin{pmatrix} 0 & -\frac{k_z}{k_t} R e^{2ik_z d} + \frac{i\Gamma_g}{k_g} S e^{(ik_z - \Gamma_g)d} \\ 0 & R e^{2ik_z d} + S e^{(ik_z - \Gamma_g)d} \end{pmatrix}, \tag{3.5}$$

where $k_g = \frac{\omega}{c}\sin\theta + g$, $g = 2\pi/\lambda_g$ with λ_g being the spatial period of the grating, $\Gamma_g = (k_g^2 - \frac{\omega^2}{c^2})^{1/2}$, $k_z = \frac{\omega}{c}\cos\theta$, $k_t = \frac{\omega}{c}\sin\theta$, and θ is the angle of incidence. The quantities R and S in Eq.(3.5) , originating respectively from the reflected and surface plasmon fields, are given as

$$R = \frac{\varepsilon k_z - i\beta}{\varepsilon k_z + i\beta} \tag{3.6}$$

$$S = \frac{2(\xi_g k_g) k_z \beta_g (1-\varepsilon)}{k_t(\varepsilon\Gamma_g + \beta_g)} \quad \frac{\beta\beta_g + \varepsilon k_t k_g}{\beta_g(\varepsilon k_z + i\beta)} , \tag{3.7}$$

where $\beta^2 = k_t^2 - \frac{\omega^2}{c^2}\varepsilon$, $\beta_g^2 = k_g^2 - \frac{\omega^2}{c^2}\varepsilon$, ξ_g is the grating amplitude and $\varepsilon = \varepsilon(\omega)$ is the frequency-dependent complex dielectric constant of the metallic grating. The plasmon resonance condition is achieved when

$$\frac{\omega^2}{c^2}\,\varepsilon_1(\omega) - k_g^2[\varepsilon_1(\omega)+1] = 0 \quad . \tag{3.8}$$

In order to completely investigate the surface effects entering into Eq.(3.4), we must know the induced molecular decay rate (γ_M) at the surface. We first give a brief review on this subject matter for the case of physisorbed molecules.

In the past two decades, there has been a large amount of effort in the study of the lifetime of an excited molecule in the vicinity of a surface,both theoretically (Kuhn, 1970; Chance et al., 1978) and experimentally (Drehage, 1974; Rossetti et al., 1980, 1982). The theoretical work has included classical reflected field theory (Kuhn, 1970) and the energy flux method (Chance et al., 1978) for both perfectly or partially reflecting flat surfaces (Philpott, 1975). The classical approaches have also been extended to the case of a rough surface including both the randomly (Arias et al., 1982) and the periodically (Leung et al., 1986, 1987b) roughened cases. These later extentions have been based on theories of image potentials for a point charge located near such surfaces as established by the Irvine group (Rahman et al., 1980a,b). Among these investigations, the general conclusion has been reached that the molecular lifetime is in general shortened due to the induced decay rate by the reflected field from the surface, and surface roughness further enhances such decay rate. Furthermore, large dependences on the orientation as well as the distance of the molecule from the surface have been observed (Chance et al., 1978).

To illustrate here how the effect of the induced decay rate (γ_M) enters into Eq. (3.4), we shall discuss γ_M for a shallow sinusoidal grating. By applying the general theory of Rahman and Maradudin (1980a), Rahman and Mills (1980b) have obtained the image potential for a point charge e near a shallow sinusoidal grating as

$$\phi(z) = -\frac{e}{8}\frac{\varepsilon-1}{(\varepsilon+1)^2}\xi_g\, g\{(\varepsilon-1)[gK_0(gz) + \frac{2}{z}K_1(gz)] + \frac{4K_1(gz)}{z}\}, \quad (3.9)$$

where K_0 and K_1 are the modified Bessel functions. For a perpendicular dipole located at (0,0,d), we can calculate the image dipole field per dipole moment from Eq. (3.9) to be (Leung et al., 1986)

$$G^R(\omega) \equiv \frac{E_\mu}{\mu} = \frac{1}{8}\frac{\varepsilon-1}{(\varepsilon+1)^2}\xi_g\, g\{g[(\varepsilon-1)(g+\frac{2}{d}) + \frac{4}{d}](gK_1 + \frac{K_0}{d})$$

$$+ \frac{4}{d^2}(\varepsilon+1)(gK_0 + \frac{3K_1}{d})\} \quad . \quad (3.10)$$

We remark that this result is first order in $\xi_g g$, in contrast to that for a randomly rough surface which has a lowest order result in $(\xi_g g)^2$ (Arias et al., 1982). Following similar steps as in Chance et al. (1978) and Arias et al. (1982), we obtain finally the γ_M on a shallow sinusoidal grating as

$$\gamma_M = \gamma_M^0[1 + \frac{3}{2}\frac{q}{k^3}\, ImG^F(1 + \frac{ImG^R}{ImG^F})] \quad , \quad (3.11)$$

where q is the quantum yield of the emitting state. $G^F(\omega)$ is the corresponding function as in Eq. (3.10) for a flat surface and is given by the Sommerfeld antenna theory as (Chance et al., 1978)

$$G^F(\omega) = -k^3 \int_0^\infty du \quad e^{-2\ell_1 \hat{d}} \frac{u^3}{\ell_1} \quad , \tag{3.12}$$

where $\hat{d} \equiv kd$, $\quad = (\ell_2 - \varepsilon\ell_1)/(\ell_2 + \varepsilon\ell_1)$, $\ell_1 = -\, i(1 - u^2)^{1/2}$ and $\ell_2 = -\, i(\varepsilon - u^2)^{1/2}$.

With $A(\omega)$ in Eq. (3.5) and γ_M in Eq. (3.11) substituted into Eq. (3.4), we have illustrated with some numerical calculations the surface effects on the direct dissociation of I_2 molecules at 4500 Å on a silver (Ag) grating with a roughness parameter $\xi_g/\lambda_g = 8 \times 10^{-3}$ (Leung et al., 1986). Figure 5 shows the distortion of the original Lorentzian line profile for different molecule-surface separations. We observe that the SP resonance (at about 2.895 eV of photon frequency) introduces a sharp edge so that the asymmetrically distorted profile shows similar behavior as for a Fano profile (Fano, 1961). Furthermore, the double-peak feature for the case of a spheroid substrate (Weitz et al., 1983) is not observed here since we have adjusted the SP resonance frequency to lie close to that of the molecular resonance. Such an adjustment is physically possible since one can vary the many parameters such as the angle of incidence (θ) and the grating period (λ_g) so that Eq. (3.8) is fulfilled for $\omega \cong \omega_M^0$. Figure 6 shows the enhancement factor versus molecule-surface distance for various incident laser frequencies . The results show clearly the existence of the critical distance (d_{cr}, below which $\sigma/\sigma_0 < 1$) and the optimal distance (d_{op}, at which

σ/σ_0 is maximum). We observe also that under the SP resonance condition, one can still have a large enhancement even at distances far from the surface. In general, the SP resonance plays a more significant role than the molecular resonance in such processes. With the existence of these distances, the experiments mentioned in the beginning of this section may be understood, at least in a qualitative manner. Furthermore, the concept of the critical distance may lead to practical applications. As an example, we suggest that if one could coat the metallic surface by means of the "fatty acid monolayer assembly technique" (Kuhn, 1968) so that all the molecules are kept at a distance above the critical distance, one could then guarantee that surface-assisted dissociation is maintained. Some future directions in this regard are mentioned in Sec. 6.

4. Line Shapes

Related to absorption/dissociation but in itself a much broader class of phenomena is that of line profiles for molecules in the vicinity of a surface. The study of such "surface distortions" of molecular line profiles can give invaluable information concerning the details of the molecular processes as well as the mechanisms by which the molecule and surface interact with each other. As already mentioned in Sec. 3, for example, the observation of the "double-peak feature" or the "sharp-edge window" in the absorption/dissociation spectrum signifies the effects of the surface plasmon on the molecular processes. In this section, we shall give a more comprehensive review of this class of phenomena.

While most of the theoretical work has been devoted to physisorbed adspicies, there has also been some work considering chemisorbed molecules (Metiu et al., 1978). In the work of Metiu and Palke (1978), the infrared

spectroscopy for the vibration of an atom chemisorbed on a solid is studied assuming a coupling between the adatom and the lattice phonons of the substrate. The analysis shows that such coupling is not sufficient to explain the large line-broadening observed experimentally (Nakata, 1976), and possible explanation is attributed instead to the coupling to the electronic degrees of freedom of the metallic substrate. Indeed, from our previous presentation in Sec. 3, we have found in a phenomenological approach that the SP coupling leads to an appreciable broadening in many cases (Nitzan et al., 1981; Leung et al., 1986) for physisorbed systems. It is therefore worthwhile to extend this previous work to the case of chemisorbed systems, first phenomenologically and then with a more thorough microscopic formalism. We are at present persuing this problem in our laboratory. For physisorbed adspieces, effects of the coupling between the system and the substrate via excitations of the electron-hole (eh) pairs, phonons and photons have been condisered for vibrational line shapes of admolecules (Gadzuk et al., 1984). Distinction between vibrational dephasing and relaxation has been emphasised in this latter work. Such vibrational dynamics has also been analyzed later in a fully quantum statistical formalism where the anharmonicity of the vibration is emphasized (Huang et al., 1985). In particular, for the system of OH on SiO_2, the dephasing rate via phonons is found to be considerably faster than the energy relaxation rate (Hutchinson et al., 1986). In addition, the vibration-rotation spectrum for physisorbed HCl on Ar(111) surface has also been investigated in a semiclassical "trajectory approach" with a collapse of the R and P band structure at low rotational energies being observed (Adams, 1986). Furthermore, aside from those phenomenological approaches

which we mentioned earlier (Nitzan et al., 1981; Leung et al., 1986), the effects of the roughness of surface on the fluoresence and absorption spectra for a molecular dipole near a randomly rough metallic surface have also been formulated in a fully quantum mechanical fashion. It was found that surface-roughness in this case induces distortions in the flat-surface Lorentzian toward a Gaussian line shape as the roughness increases (Agassi, 1986). However, it was criticized earlier that these vibrational spectra of coupled adsorbed molecules may not be Lorentzian to start with,even in the flat surface case (Langreth, 1985; Sorbello, 1985). In a very clever analysis, Langreth (1985) has shown that the line shape for an isolated vibrational mode of adspecies on a metallic surface is necessarily asymmetric in the presence of the damping, where the profile is more of the Fano type (Fano, 1961) than the Lorentz type. This is a good example showing that the study of line profiles can lead to an understanding of the coupling mechanism between the molecule and the surface.

Aside from vibrational and rotational spectra, electronic and desorption spectral line shapes are also of great interest. In particular, electronic excitation by a UV-visible laser leading to desorption of an admolecule has been recently studied by Lin et al (1987a). The result shows that the laser-stimulated desorption (LSD) spectra (LSD yield vs laser frequency) exhibit the well known Beutler-Fano (Fano, 1961) behavior due to the configuration interaction between the molecular excited electronic states and the desorption continuum. These investigators have also studied the case of IR LSD spectra (Lin et al., 1987b), where the same Beutler-Fano line shape is found to exist due to the coupling between the intramolecular optically pumped vibrational modes and the desorption continuum. The

effects of inhomogeneous broadening on these IR LSD line shapes have also been investigated (Gortel et al., 1986; Lin et al., 1987b). Because of the heterogeneity due to different adsorption sites and imperfections in the underlying substrate,strong asymmetry and double-peak features in the absorption spectrum have been reported.[64] In case when optical vibrational modes are involved, the LSD spectra can be analyzed as a superposition of Beutler-Fano bands (Lin et al., 1987b).

In spite of the numerous studies of surface effects on the absorption spectra of admolecules, it appears, in all the previously mentioned references, that the free line profile (i.e., the absorption line profile for a free molecule in the absence of the surface) has almost always been assumed to be symmetric, often of a Lorentzian type, so that asymmetric distortions are brought about by the presence of the surface. There remains therefore one whole class of problem previously uninvestigated, namely that when the free line profile is already asymmetric in nature. This would include, for example, processes like autoionization and predissociation in molecular systems. In a recent work (Leung et al., 1987), we have reported some preliminary results in this direction based on an extention of our previous work in the distortions of the Lorentzian profile on top of a silver grating (Leung et al., 1986), which we now describe below.

In analogue to the "driven damped oscillator model" (Eq.(3.1)) which describes a free Lorentzian profile in the absence of surface effects, we have adopted the mechanical model recently proposed by Sorbello (1985) to describe the asymmetric Fano (1961) effect. The model consists of the coupling of a normal mode (ω_0) to a lossy broad-band system such as a viscous bath, with both the oscillator and the bath being described by one

degree of freedom. The line-shape function obtained in this model can be reexpressed in the form*

$$I_0(\omega) = \frac{(q+\varepsilon_0)^2}{1+\varepsilon_0^2}\,\sigma_0(\omega) \quad , \tag{4.1}$$

where q is the asymmetric profile index depending on the ratio of the driving force on the oscillator to that on the bath, and $\sigma_0(\omega)$ is the background intensity due to direct excitation of the bath. The reduced energy variable ε_0 in Eq. (4.1) is expressed as

$$\varepsilon_0 = \frac{2(\omega-\omega_0-\Delta\omega_0)}{\gamma_0} \quad , \tag{4.2}$$

where $\Delta\omega_0$ and γ_0 are the level shift and decay rate of the system , respectively. In general, $\Delta\omega_0 << \omega_0$, and hence

$$\varepsilon_o \cong \frac{2\Delta\omega}{\gamma_0} \tag{4.3}$$

with $\Delta\omega = \omega - \omega_0$.

In an analogous way as for the "distorted Lorentzian profile" (Eq.(3.4)), we have obtained the surface distorted Fano profile in the form

$$I(\omega) = \frac{(q+\varepsilon)^2}{1+\varepsilon^2}\,\left|\hat{n}_\mu\cdot[1+A]\cdot\hat{n}\right|^2\,\sigma(\omega) \quad , \tag{4.4}$$

* We have changed some of Sorbello's (1985) original notation. Here we denote every quantity which refers to the free molecule case in the absence of the surface by the subscript "0".

where now

$$\varepsilon = \frac{2\Delta\omega}{\gamma} \quad . \tag{4.5}$$

Here all quantities without a subscript '0' refer to those at the surface, and we have neglected the effect of the surface on q and ω_0 (Leung et al., 1987). We have also assumed the substrate to be a shallow sinusoidal grating, and hence the quantities $A(\omega)$ and γ are given as before in Eqs.(3.5) and (3.11) for a molecular dipole located at (0,0,d) and perpendicular to the surface. With some reasonable forms for $\sigma_0(\omega)$, we have examined the surface distortions for the cases of certain autoionization and predissociation absorption spectra, where results are shown in Figs. 7 and 8, respectively. From these preliminary results basing on such model studies, we observe the familiar double-peak features and the broadening of the oringinal profile window at the steep edge near the low-frequency end, while at the high frequency end of the distorted profile, the surface plasmon resonance leads to a new window. Furthermore, we observe that at such molecule-surface distances (d ~ 500 Å) under the model calculation conditions, a surface enhancement effect is in general observed, implying that enhanced molecular photo-predissociation may also be possible, provided that the molecule is not located too close to the surface and the resonant plasmon field decays very slowly in the direction normal to the surface. It has been argued previously that due to the "slow nature" (on a time scale of $\sim 10^{-9}$ s) of these unimolecular processes such as predissociation, the surface enhancement effects can hardly be effective due to the large induced

molecular decay rate caused by the presence of the surface (Chuang, 1982). However, as seen from our preliminary model study, such an argument is not conclusive since there are many parameters (e.g., degree of the roughness, angle of incidence, etc.) that one can adjust, so that the molecule can still experience a large enhanced field at a distance relatively far from the surface at which the induced decay rate is of minor consequence. Thus, it would be interesting to conduct a more detailed study of such possible enhanced "slow processes". The practical realization of these ideas in actual gas-surface systems might lead to the development of a new kind of photochemistry, namely, laser-assisted heterogeneous catalysis (Lin et al., 1984) via surface predissociation of physisorbed molecule, so that the problem of desorption of the reaction products from the surface can almost be completely ignored. We should also add that possible enhanced molecular predissociation has been examined recently by means of yet a different mechanism, namely, surface magnetic field/laser synergistic effects (Bhattacharyya et al., 1981, 1982). In contrast to the SP- enhanced pumping rate of the absorption/dissociation process discussed here, this latter mechanism creates its own dissociation channels via crossings between the ground and continuum electronic potential surfaces due to the photon-dressed effect associated with the ground state, and the Zeeman splitting of the continuum levels.

5. Laser-Induced Deposition

A relatively new field has emerged in which a low-power laser is used to enhance deposition of a metal on a surface, generally semiconductor. The archetypal experiment involves a weak 257 nm cw laser (1 - 10 W/cm^2)

irradiating a SiO_x surface under an organometallic gas ($Cd(CH_3)_2$ at 1 torr pressure (Brueck et al., 1982), for example. A closely related subject, but one which is in many ways similar, is the topic of laser-induced damage at surfaces. This has been studied much more extensively (Fauchet et al., 1982; Sipe et al., 1983). We shall find that the deposition problem is simpler in that the relevant chemistry appears to take place well above the surface, and hence the Rayleigh expansion can be used to calculate the field strengths.

The common thread between these two problems is the interaction between the laser and the surface. Here primarily two effects predominate: laser heating and the excitation of surface plasmons. Sometimes both effects are important, though in our deposition example, the surface heating amounts to only about 1 K. In general, however, given the interaction between the surface and laser, several mechanisms can occur:

1) The laser can melt the surface, and then the plasmon or diffusive motion along the surface creates a standing wave in the molten substance. Upon cooling this pattern is frozen into the surface (Fauchet et al., 1982; Ehrlich et al., 1983; Osgood et al., 1982; Chen et al., 1985).
2) The laser can heat an adsorbed layer (as opposed to the true surface) and cause rearrangement. This has been observed with copper deposition on silica surfaces (Moylan et al., 1986; Ehrlich et al., 1983; Osgood et al., 1982; Chen et al., 1985).
3) The laser can affect the adsorption process itself. This can happen either by the enhancement of the adsorption process because of the

laser (we are unaware of any experimental evidence for this occuring), or the laser can enhance the dissociation of the molecular precursors to adsorption. Brueck and Ehrlich's experiment appears to be an example of this latter phenomenon.

Sipe, Young, Preston and van Driel (1983) have written extensively on the first process. To account for this phenomena, it is essential to know the field intensities at the surface. As mentioned in Sec. 1, this is a very complicated problem. They have calculated the energy deposition (due to the laser) just below the surface and then used a variational calculation to compute the local field strengths near the surface. Moylan, Baum and Jones (1986) have discussed the second possibility and have related the grating growth rate to the focal point size of the laser, along with the diffusion coefficient of the adsorbed layer. They are then able to generate the kinetic equations for motion along the surface.

The primary subject of this section will be to discuss the third process, namely, we shall try to account for the observations of Brueck and Ehrlich (1982). These results are more fully described in Jelski and George (1987). Put briefly, the laser, in this case weak so as to minimize surface heating, causes a resonant plasmon due to coupling with the surface roughness. This plasmon enhances the dissociation of the inorganic precursor above the surface, but since the field strength is spatially periodic, this leads to periodic deposition.

A theoretical treatment of this process requires two steps. In the first step, we need a simple method to calculate the field strength; the difficulties involved here have been discussed in Sec. 2. We note here that

the problem is enormously simplified by the fact that dissociation takes place well above the surface (see Sec. 3). This permits use of the Rayleigh expansion, which is exact above the selvedge region. Secondly, we want a fast calculation of the field strength since our problem requires this strength as a function of grating wavenumber and grating height. The approximation of Jelski and George (1987) described in Sec. 2 seems most appropriate to our problem since, in every case, we require the intensity of only the resonant frequency. A general reflectivity calculation is not called for.

Thus, stated explicitly, our method is as follows:

1) We assume (see Jelski et al. (1987b) for a more complete discussion) that the enhanced deposition is due to the fact that the plasmon field enhances the dissociation of the adspecies precursor.
2) This dissociation takes place well above the surface (see Sec. 3), thus permitting the use of the Rayleigh expansion. We use the approximation of Jelski and George to calculate this.
3) To simplify the calculation, we assume that the dissociation cross-section of the precursor is proportional to the field intensity and that the deposition rate is proportional to the dissociation rate. The first approximation breaks down for strong fields, whereas the second fails for high pressures.
4) Finally, we assume that the final grating profile is sinusoidal. This will turn out to be approximately accurate, and we shall see from the calculation that it can be corrected, at the cost of considerably more complexity.

Our model will be the experiment of Brueck and Ehrlich (1982). We shall assume a cadmium thin layer with a dielectric constant of -2.5 + 1.3i. Dimethyl cadmium gas at ~ 1 torr pressure and at room temperature is above the surface. A 257 nm laser at 10 W/cm^2 is irradiating the system. The dissociation cross-section of

$$Cd(CH_3)_2 + h\nu \rightarrow Cd + 2CH_3 \tag{5.1}$$

will be denoted by σ_k, and hence

$$\frac{d[Cd]}{dt} = \sigma_k E_k^2 \equiv \sigma_k I(k) \quad , \tag{5.2}$$

where E is the field strength and I is the intensity. The subscript k refers to the wavenumber of the incident light.

Before going further, we note that cadmium is a lossy substance with a large imaginary part to the dielectric constant. Hence the flat surface dispersion relation, given by Eqs. (2.30) or (3.8), is inappropriate since it assumes that ε_2 is small. We thus need to reconsider the flat surface case when ε_2 cannot be so considered. From Eq. (2.29), and noting that $\xi_0 = 0$, to first order in ξ_1 we get

$$A_1 \approx \frac{\mu_1 E_i}{M_{11}} = \frac{i(\alpha_0\beta_1 - k_0k_1)(\varepsilon\alpha_1 - \beta_1)\xi_1 E_i}{\varepsilon k^2 - k_1^2(1+\varepsilon)} \quad . \tag{5.3}$$

This is the shallow grating limit result previously derived (Maradudin, 1982; Jha et al., 1980), which is identical, except for notation, to Eq. (3.7). Since this is an expansion only to first order in ξ_1, it is valid only for shallow gratings. Let us denote the denominator by R. Then if

$$R \equiv \epsilon k^2 - k_1^2(1+\epsilon) = 0 \quad , \tag{5.4}$$

A_1 becomes large and resonant. This leads to the resonance condition

$$k_1^2 = k^2 \frac{\epsilon_1}{\epsilon_1 + 1} \quad , \tag{5.5}$$

where ϵ_1 is the real part of ϵ. Equation (5.5) is essentially the condition expressed in Eq. (3.8) and is valid if ϵ_2 is small. If that is not the case, then Eq. (5.4) will never hold and instead we have to minimize R^2. This yields

$$|R|^2 = [k_g^2(1+\epsilon_1) - k^2\epsilon_1]^2 + [\epsilon_2(k_g^2 - k^2)]^2 \quad , \tag{5.6}$$

or upon setting the derivative equal to zero,

$$k_g^2 = \frac{k^2[\epsilon_1(1+\epsilon_1) - \epsilon_2^2]}{(1+\epsilon_1)^2 + \epsilon_2^2} \quad . \tag{5.7}$$

Equation (5.7) reduces to Eq. (5.4) as $\epsilon_2 \to 0$.

As the grating becomes deeper, R also depends on powers of ξ_m. But in general, we can express the resonance condition by

$$\frac{d|R|}{dk_1} \equiv R' = 0 \quad . \tag{5.8}$$

For very deep gratings this may not be quite sufficient, as we would also need to account for the behavior of the numerator, although for our purposes here it is sufficient.

Figure 9 shows the resonance factor, $|R|$, as a function of grating wavenumber for the model cadmium surface. For the shallow grating (1 nm) the resonance is well defined. As the grating deepens it becomes apparent that the resonance is less and less pronounced.

Figure 10 is a graph of R' vs. grating wavenumber. Here two things can be seen: one is that as the grating gets deeper then the resonance frequency (where the curves cross zero) shifts toward higher frequencies. This precludes any grating from growing sinusoidally, for as the grating gets larger the wavelength gets shorter. Nevertheless, we can approximate our grating as sinusoidal since the shift is relatively small.

Secondly, we note that the 24 nm curve never crosses zero. Hence there is no resonance at all. This means that grating growth will stop. This does not imply that deposition will stop, but only that deposition will occur evenly across the surface, i.e., our thin layer will get thicker. Hence peaks and valleys will grow identically. We can already predict the maximum grating height, namely 48 nm (2 × the amplitude). This is

approximately half of what Brueck and Ehrlich (1982) observe. This error may be due to our approximate (and frequency-independent) form for the dielectric constant, our ignoring thin layer effects, or our approximate form for the Rayleigh expansion.

Having determined the maximum grating height, we now need to determine the rate of grating growth. Hence we must ask the question "How much more resonant is a given frequency than its neighbors?" In a word, we want to know the concavity of the curves in Fig. 9. Let us define

$$G(k_r,\xi) \equiv \left(\frac{\partial^2 R}{\partial^2 k_g^2}\right)_{k_g=k_r} , \tag{5.9}$$

where k_r is the resonant frequency determined by Eq. (5.8). As the resonance disappears the concavity goes to zero.

Let us assume a sinusoidal grating of amplitude ξ, with N as the number of cadmium atoms that adsorb at the peak. Then we can write

$$\frac{d\xi}{dt} = \frac{d\xi}{dN}\frac{dN}{dt} \tag{5.10}$$

where

$$\frac{d\xi}{dN} = \frac{Mk_g}{2\rho y} , \tag{5.11}$$

M is the atomic mass of cadmium, ρ is the density of metallic cadmium and y is the dimension of the surface (parallel to the grooves).

The rate dN/dt is proportional to right-hand side of Eq. (5.2), i.e., to the number of Cd atoms that adsorb on the surface. We will denote the sticking coefficient by the letter a. Then

$$\frac{dN}{dt} = a\sigma_k I(k,r)G(k_r,\xi) \tag{5.12}$$

where r is the spatial variation of the intensity. The quantity $G(k_r,\xi)$ weights the function according to the frequency variation of the resonance. Equation (5.12) can be integrated to yield $\xi(t)$. Choosing the constants to reflect the time span of Brueck and Ehrlich's experiment, we generate the function shown in Fig. 11.

Thus we have developed a simple model to account for the chemical vapor deposition phenomena. We have assumed that the ultimate cause of this effect is the laser-induced plasmon which enhances dissociation above the surface. We have succeeded in qualitatively reproducing Brueck and Ehrlich's experiments. A more sophisticated approach will have to allow for the thin layer effect, provide a more accurate function for the dielectric constant, relieve the condition that the grating be sinusoidal, and perhaps use the full Rayleigh expansion rather than the approximate form.

6. Conclusion

In this paper, we have presented a review of different types of photochemical processes at rough (metallic) surfaces, giving attention to the work done by others as well as by our group. In contrast to a previous review article by Harris and coworkers (Goncher et al., 1984) which emphasizes experimental studies in photodissociation processes, our present

article emphasizes the theoretical aspects and incorporates also phenomena like molecular lineshapes and dposition on rough surfaces. Since we have been following the classical phenomenological treatment (Maxwell's theory) for the surface fields, we have also provided the mathematical basis (Sec. 1) that clarifies the foundation of the Rayleigh expansion which has been found invaluable in the treatment of surface EM fields.

The main physical mechanism involved in all the processes we have discussed has been the surface plasmon effect. This has turned out to be the case since we have assumed physisorbed systems throughout. For chemisorbed systems, bond-formation effects will arise between the admolecule and the surface, and charge-transfer processes should be given equal importance as the SP effect. We hope to generalize our previous work in this direction in the future. Such generalization may also find applications in the theoretical exploration of possible laser-assisted heterogenous catalysis as well as deeper understanding of the deposition process discussed in Sec. 4, which has hitherto been treated only phenomenologically. Furthermore, we have in this review assumed an isolated molecule-surface system. An actual physical situation will mor generally involve an ensemble of molecules in the vicinity of the surface. We therefore also plan to investigate in the future the effects of the neighboring admolecules on the phenomena reviewed in Secs. 3 to 5.

Finally, it is clear in this review on surface photochemistry that all the analysis is based on the linear Maxwell's theory. Since nonlinear optical surface processes have attracted much attention recently (Chen et al., 1981), we feel that the time is ripe to look into other possible

photochemical processes exploiting these nonlinear optical techniques. We have begun our first attempt to reinvestigate the above processes on a phase-conjugated surface, replacing the ordinary substrate metallic surface by an optically nonlinear substrate such as GaAs(110). Some interesting preliminary results have been obtained with respect to the linewidth and lifetimes for molecules near such conjugated surfaces (Lin et al., 1987). We believe that it would be very worthwhile to invest more efforts in this direction in the future.

Acknowledgments

This research was supported by the Office of Naval Research, Air Force Office of Scientific Research (AFSC), United States Air Force, under Contract F49620-86-C-0009, and the National Science Foundation under Grant CHE-8620274. The United State Government is authorized to reproduce and distribute reprints for governmental purposes notwithstanding any copyright notation hereon.

References

Adams, J.E., 1986, J. Chem. Phys. 84, 3589.

Agassi, D., 1986, Phys. Rev. B 33, 3873.

Agassi, D. and George, T.F., 1986a, Phys. Rev. B 33, 2393.

Agassi, D. and George, T.F., 1986b, Surf. Sci 172, 230.

Arias, J., Aravind, P.K. and Metiu, H., 1982, Chem. Phys. Lett. 85, 404.

Avouris, P. and Peterson, B.N.J., 1984, J. Phys. Chem. 88, 837.

Bhattacharyya, D.K., Lam, K.S. and George, T.F., 1981, J. Chem. Phys. 75, 203.

Bhattacharyya, D.K., Lin, J. and George, T.F., 1982, Surf. Sci. 116, 423.

Bourdon, E.B.D., Cowin, J.P., Harrison, I., Polanyi, J.C., Segner, J., Stanners, C.D. and Young, P.A., 1984, J. Phys. Chem. 88, 6100.

Bourdon, E.B.D., Das, P., Harrison, I., Polanyi, J.C., Segner, J., Stanners, C.D., Williams, R.J. and Young, P.A., 1986, Faraday Disc. Chem. Soc. 82, paper 20.

Brueck, S.R.J. and Ehrlich, D.J., 1982, Phys. Rev. Lett. 48, 1678.

Chance, R.R., Prock, A. and Silbey, R., 1978, Adv. Chem. Phys. 37, 1.

Chang, R.K. and Furtak, T.E., ed., 1982, Surface Enhanced Raman Scattering, Plenum, New York.

Chen, C.K., de Castro, A.R.B. and Shen, Y.R., 1981, Phys. Rev. Lett. 46, 145.

Chen, C.J. and Osgood, R.M., 1983, Phys. Rev. Lett. 50, 1705.

Chen, C.J., Gilgen, H.H. and Osgood, R.M., 1985, Opt. Lett. 10, 173.

Chuang, T.J., 1982, Surf. Sci. Rep. 3, 1.

Cline, M.P., Burber, P.W. and Chung, R.K., 1986, J. Opt. Soc. Am. B 3, 15.

Drehage, K.H., 1974, Progress in Optics XII, ed. by E. Wolf, North-Holland, Amsterdam, p. 165 ff.

Ehrlich, D.J. and Osgood, R.M., 1981, Chem. Phys. Lett. 79, 381.

Ehrlich, D.J. and Tsao, J.Y., 1983, J. Vac. Sci. Technol. B 1, 4, 969.

Equiluz, A.G. and Maradudin, A.A., 1983, Phys. Rev. B 28, 711.

Fano, U., 1941, Opt. Soc. Am. 31, 213.

Fano, U., 1961, Phys. Rev. 124, 1866.

Fauchet, P.M. and Siegman, A.E., 1982, Appl. Phys. Lett. 40, 824.

Feibelman, P.J., 1982, Prog. Surf. Sci. 12, 287.

Fleischmann, M., Handra, P.J. and McQuillan, A.J., 1974, Chem. Phys. Lett. 26, 163.

Gadzuk, J.W. and Luntz, A.C., 1984, Surf. Sci. 144, 429.

Garoff, S., Weitz, D.A. and Alverz, M.S., 1982, Chem. Phys. Lett. 92, 283.

George, T.F., 1982, J. Phys. Chem. 84, 10.

Gersten, J.I. and Nitzan, A., 1985, Surf. Sci. 158, 165.

Glass, N.E. and Maradudin, A.A., 1981, Phys. Rev. B 24, 595.

Glass, N.E., Weber, M. and Mills, D.L., 1984, Phys. Rev. B 29, 6548.

Goncher, G.M., Parsons, C.A. and Harris, C.B., 1984, J. Phys. Chem. 88, 4200.

Gortel, Z.W., Piercy, P., Teshima, R. and Kreuzer, H.J., 1986, Surf. Sci. 165, L12.

Huang, X.Y., George, T.F. and Yuan, J.M., 1985, J. Opt. Soc. Am. B 2, 985.

Hutchinson, M. and George, T.F., 1986, Chem. Phys. Lett. 124, 211.

Jelski, D.A. and George, T.F., 1987a, J. Phys. Chem. 91, 3779.

Jelski, D.A. and George, T.F., 1987b, J. Appl. Phys. 61, 2353.

Jha, S.S., Kirtley, J.R. and Tsang, J.C., 1980, Phys. Rev. B 22, 3973.

Kuhn, H., 1968, Structural Chemistry and Molecular Biology, ed. by A. Rich and N. Davidson, Freeman, San Francisco, p. 566 ff.

Kuhn, H. 1970, J. Chem. Phys. 53, 101.

Laks, B., Mills, D.L. and Maradudin, A.A., 1981, Phys. Rev. B 23.

Langreth, D.C., 1985, Phys. Rev. Lett. 54, 126.

Lee, K.T. and George, T.F., 1985, Phys. Rev. B 31, 5106.

Leung, P.T. and George, T.F., 1986, J. Chem. Phys. 85, 4729.

Leung, P.T. and George, T.F., 1987a, Chem Phys. Lett. 134, 375.

Leung, P.T., Wu, Z.C., Jelski, D.A. and George, T.F., 1987b, Phys. Rev. B 36, 1475.

Lin, J.T., Murphy, W.C. and George, T.F., 1984, Ind. Eng. Chem. Prod. Res. Dev. 23, 334.

Lin, J.T., Huang, X.Y. and George, T.F., 1987, J. Opt. Soc. B 4, 219.

Lin, S.H., Boeglin, A., Fain, B. and Yeh, C.Y., 1987a, Surf. Sci. 180, 289.

Lin, S.H., Boeglin, A. and Fain, B., 1987b, J. Opt. Soc. Am. B 4, 211.

Lundquist, B.I., 1984, Many-Body Phenomena at Surfaces, ed. by P. Langreth and H. Suhl, Academic, Orlando, p. 93 ff.

Maradudin, A.A. and Mills, D.L., 1975, Phys. Rev. B 11, 1392.

Maradudin, A.A., 1982, Surface Polaritons, ed. by V.M. Agranovich and D.L. Mills, North-Holland, Amsterdam, Chapt. 10.

Marvin, A., Toigo, F. and Celli, V., 1975, Phys. Rev. B 11, 2777.

McCall, S.L. and Platzman, P.M., 1980, Phys. Rev. B 22, 1660.

Meier, M., Wokaun, A. and Liao, P.F., 1985, J. Opt. Soc. Am. B 2, 931.

Metiu, H. and Palke, W.E., 1978, J. Chem. Phys. 69, 2574.

Moskovits, M., 1985, Rev. Mod. Phys. 57, 783.

Moylan, C.R., Baum, T.H. and Jones, C.R., 1986, Appl. Phys. A 40, 1.

Murray, C.A., include Ref. 29, p. 203 ff.

Nakata, T., 1976, J. Chem. Phys. 65, 487.

Nitzan, A. and Brus, L.E., 1981, J. Chem. Phys. 74, 5321 and 75, 2205.

Osgood, R.M., Jr. and Ehrlich, D.J., 1982, Opt. Lett. 7, 385.

Petit, R., 1980, Electromagnetic Theory of Gratings, ed. by R. Petit, Springer-Verlag, Berlin, Chapt. 1.

Philpott, M.R., 1975, J. Chem. Phys. 62, 1812.

Rahman, T. and Maradudin, A.A., 1980a, Phy. Rev. B 21, 504.

Rahman, T. and Mills, D.L., 1980b, Phys. Rev. B 21, 1432.

Rayleigh, J.W.S., 1907, Proc. Roy, Soc. A 79, 399.

Rossetti, R. and Brus, L.E., 1980, J. Chem. Phys. 73, 572.

Rossetti, R. and Brus, L.E., 1982, J. Chem. Phys. 76, 1146.

Sheng, P., Stepleman, R.S. and Sanda, P.N., 1982, Phys. Rev. B 26, 2907.

Sipe, J.E., Young, J.F., Preston, J.S. and van Driel, H.M., 1983, Phys. Rev. B 27, 1141.

Sorbello, R.S., 1985, Phys. Rev. B 32, 6294.

Toigo, F., Marvin, A., Celli, V. and Hill, N.R., 1977, Phys. Rev. B 15, 5618.

Weber, M.G., 1986, Phys. Rev. B 33, 9.

Weitz, D.A., Garoff, S., Gersten, J.I. and Nitzan, A., 1983, J. Chem. Phys. 78, 5324.

Height (nm)	R (exact)	R (Weber's method)	Error (%)
50	0.855	0.856	0.117
100	0.566	0.570	0.707
200	0.163	0.155	4.91
300	0.184	0.158	14.1
400	0.298	0.273	8.39
500	0.380	0.363	4.47
600	0.422	0.413	2.13

Table 1. Percentage error of Weber's mode-coupling perturbation calculation: reflectivity versus height over the range of grating heights for which the exact theory (undressed) converges. Frequency and angle (2.215 eV and 32°) were chosen so that that the minigap region of the surface polariton dispersion curve is being probed. The surface is a silver sawtooth grating with a wavelength of 8000 Å. (This table is reproduced from Weber (1986) with permission of the author.)

FIGURE CAPTIONS

1. Reflectivity as a function of photon energy of the sawtooth profile grating for two values of the grating height h. The solid line is the exact result and the dashed line is the perturbation theory result. In the first graph, the two curves are coincident to within graphical accuracy. The second graph is done for the maximum grating height for with the exact theory converges. (Reproduced from Weber (1986) with permission of the author.)

2. Plot of the plasmon field strength (A_1) calculated from Eq. (2.26) using the dressed Rayleigh expansion described in the text. This is compared with the exact calculation. The dielectric constant used is -2.5 + 1.3i, the incident light has a wavelength of 257 nm, and the grating wavenumber is taken as 2.95×10^7 m^{-1}.

3. Geometrical arrangement of the photodissociation process.

4. (a) Sinusoidal grating. The cross-hatched area represents the metal. (b) Square-well grating showing a separation into three layers, one of which is periodic in the x-direction and two of which are uniform. (c) Generalization of the square-well grating in which there are three periodic layers.

5. Distortion of the Lorentzian line profile for various molecule-surface distances for a perpendicular molecular dipole. The system consists of an I_2 molecule on a silver sinusoidal grating. We refer to the text for numerical data.

6. Enhancement factor vs. molecule-surface distance for various incident laser frequencies. (a) E_γ = 2.895 eV (at plasmon resonance); (b) E_γ = 2.5 eV; and (c) E_γ = 2.755 eV (at molecular resonance). Other parameters are the same as in Fig. 4.

7. Distortion of the Fano profile with $\sigma_0(\omega)$ a constant which simulates certain autoionization processes. The profile constants are $\gamma_0 = 5 \times 10^2$, $\omega_0 = 1.6 \times 10^4$ and $q = -2.65$. Note that the scales for $I_0(\omega)$ and $I(\omega)$ are different. The y-axis quantities are in arbitrary units.
8. Distortion of the Fano profile with $\sigma_0(\omega) = 1/\omega^2$ which simulates certain predissociation processes. The profile constants are $\gamma_0 = 4 \times 10^3$, $\omega_0 = 1.17 \times 10^4$ and $q = 3.0$. The y-axis quantities are in arbitrary units.
9. Grating wavenumber vs. the value of the resonance factor for different grating amplitudes.
10. Value of R' vs. grating wavenumber for different grating amplitudes. Note the frequency shift in the resonance frequency and that for $\xi \geq 24$ nm there is no resonance frequency.
11. The dynamics of grating growth: time vs. grating amplitude.

Fig 1

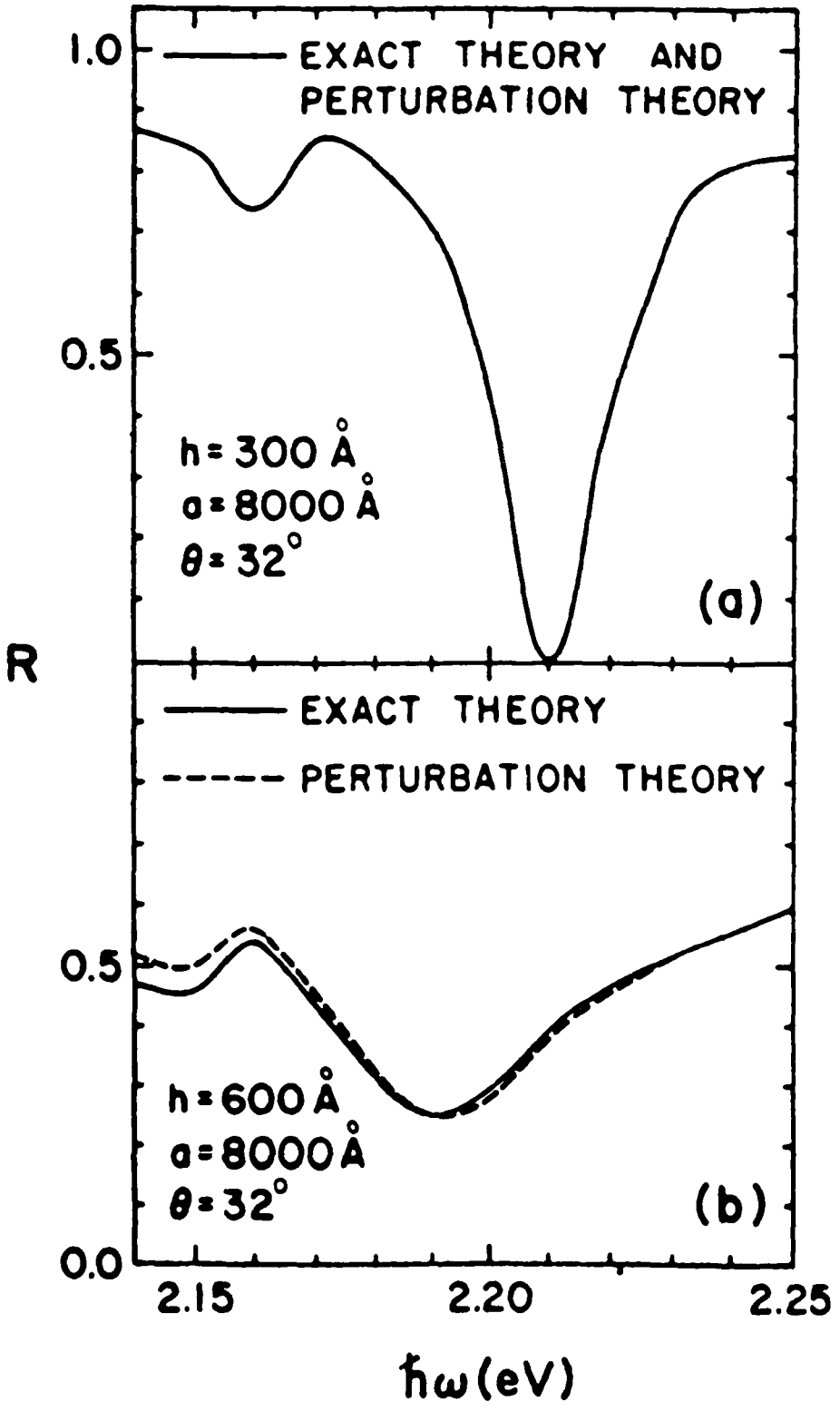
1.0
0.5
EXACT THEORY AND
PERTURBATION THEORY
h = 300 Å
a = 8000 Å
θ = 32°
(a)
R
EXACT THEORY
PERTURBATION THEORY
0.5
h = 600 Å
a = 8000 Å
θ = 32°
(b)
0.0
2.15
2.20
2.25
ħω (eV)

Fig. 2

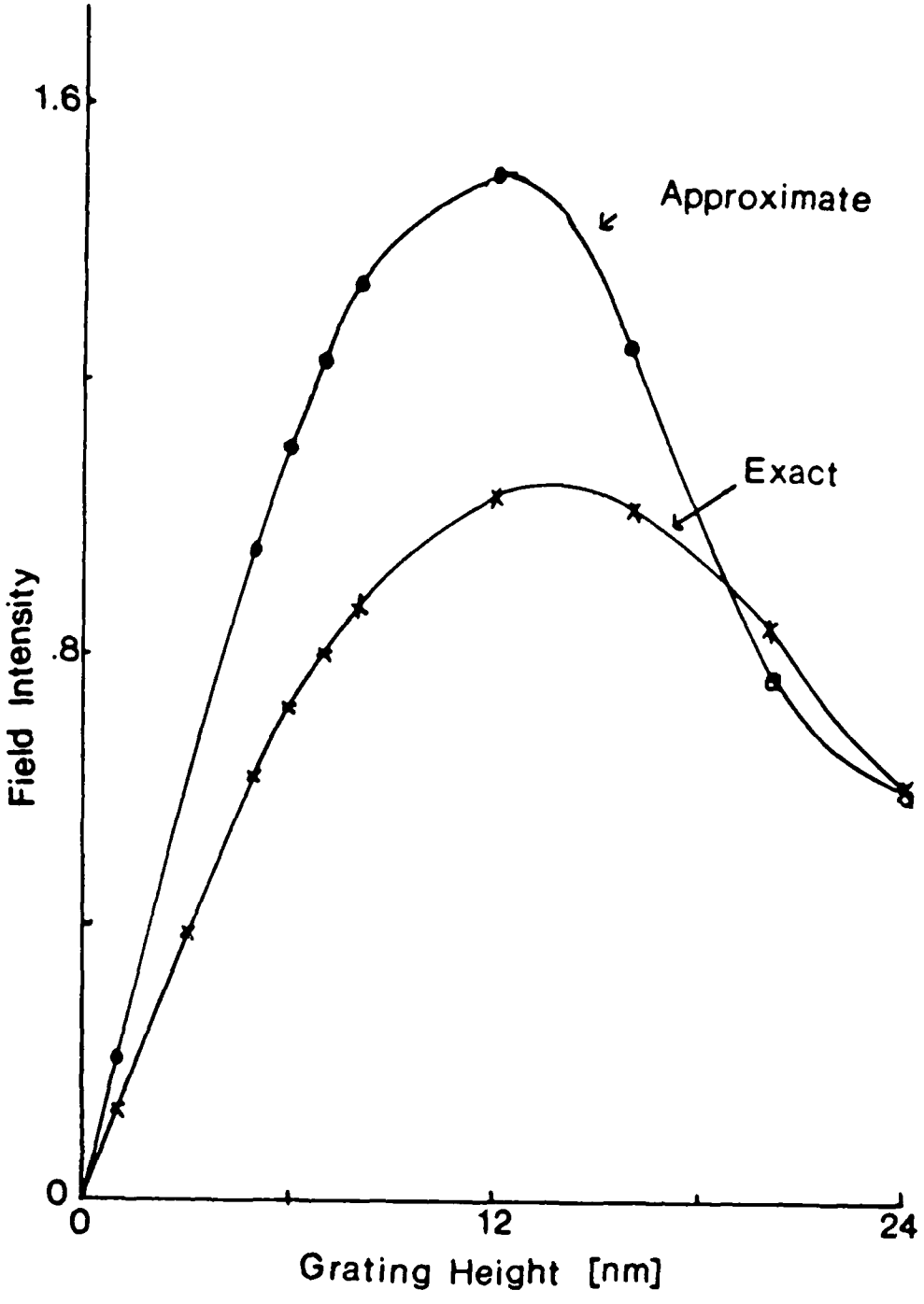
1.6
.8
0
Field Intensity
Approximate
Exact
0
12
24
Grating Height [nm]

Fig. 3

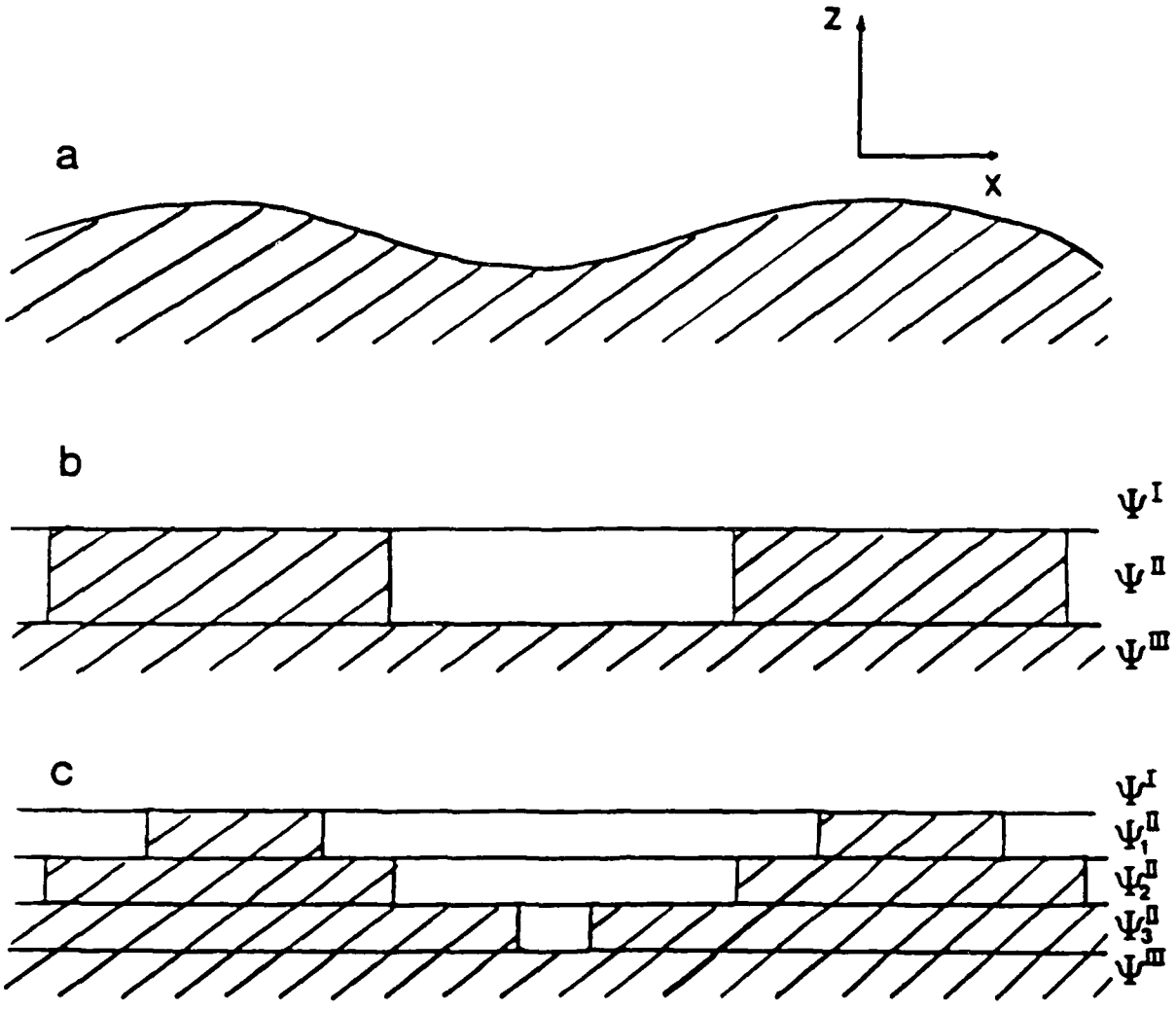

Fig 4

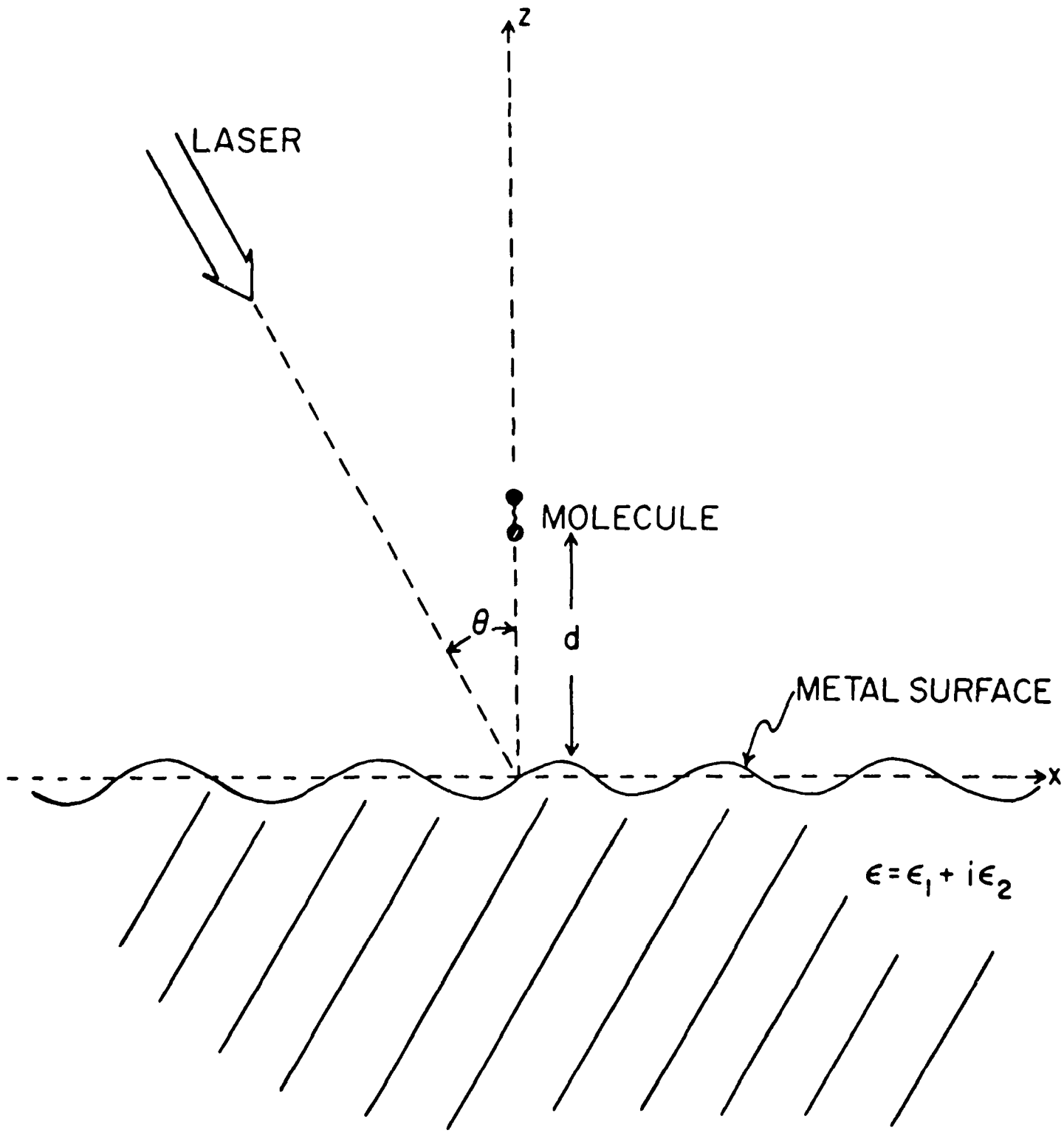

Fig. 5

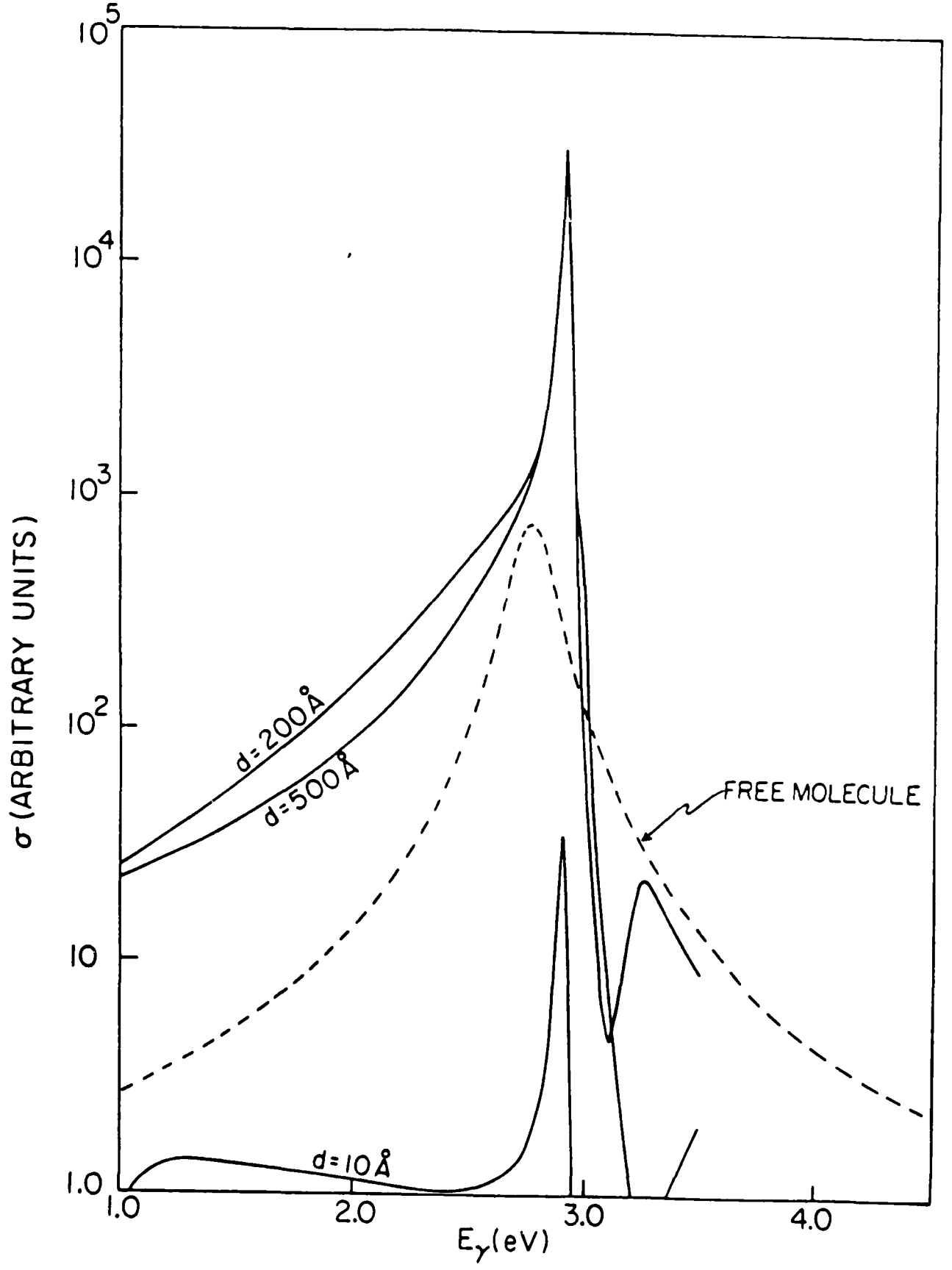
10^5
10^4
10^3
10^2
10
1.0
σ (ARBITRARY UNITS)
d=200Å
d=500Å
d=10Å
FREE MOLECULE
1.0
2.0
3.0
4.0
E_γ(eV)

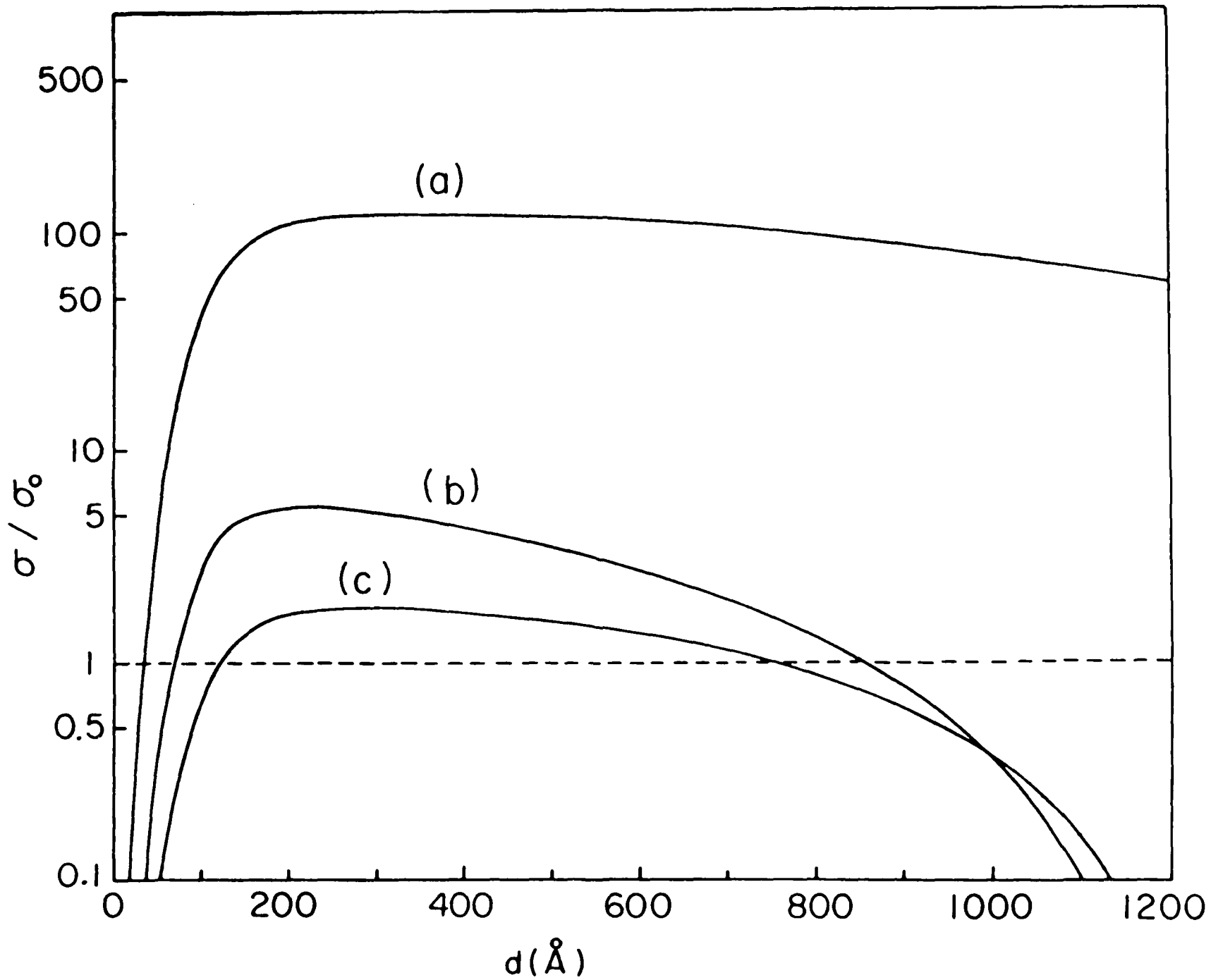
500
100
50
10
5
1
0.5
0.1
σ / σ°
(a)
(b)
(c)
0
200
400
600
800
1000
1200
d(Å)

Fig. 7

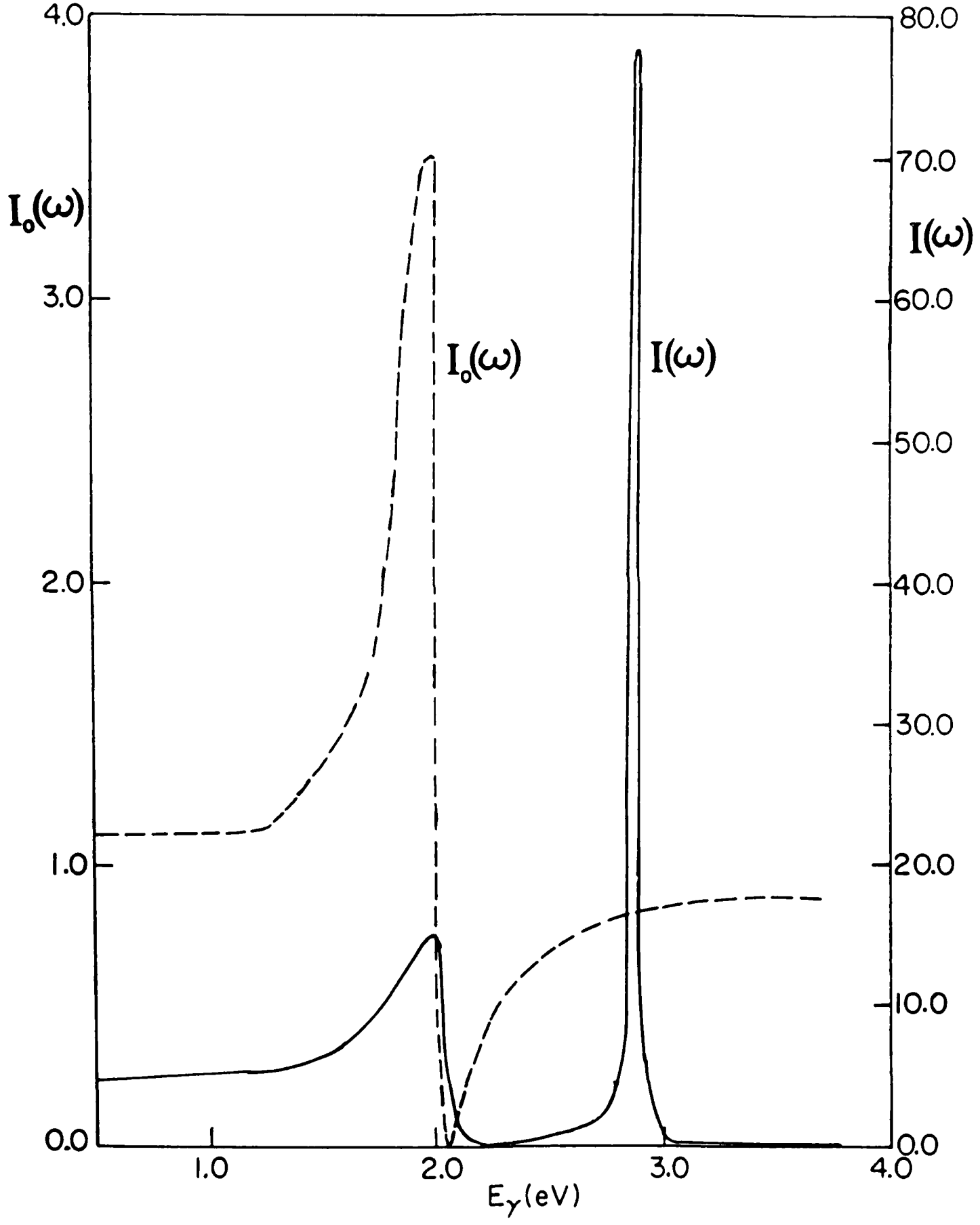
4.0
3.0
2.0
1.0
0.0
$I_o(\omega)$
80.0
70.0
60.0
50.0
40.0
30.0
20.0
10.0
0.0
$I(\omega)$
$I_o(\omega)$
$I(\omega)$
1.0
2.0
3.0
4.0
E_γ(eV)

Fig 8

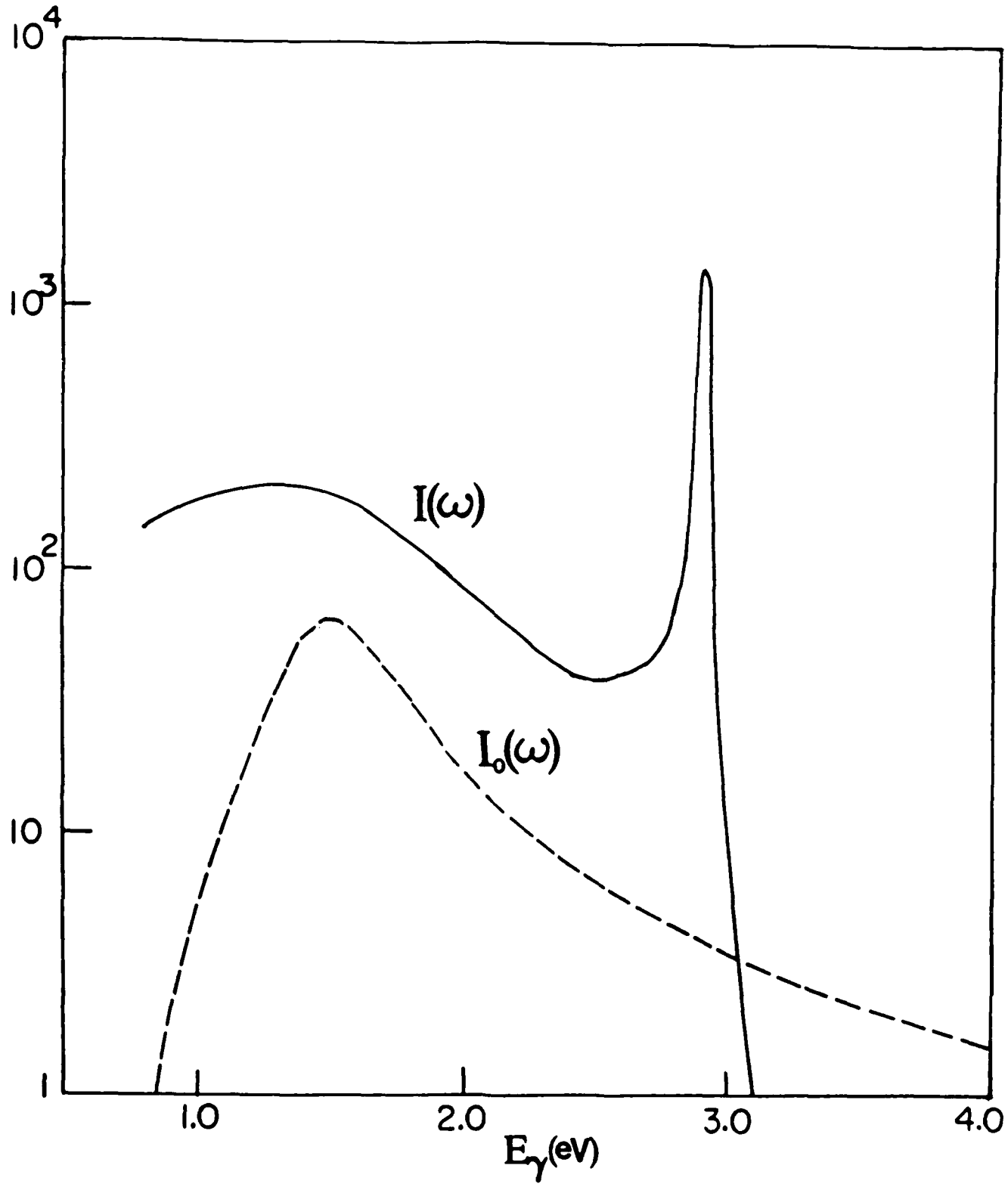

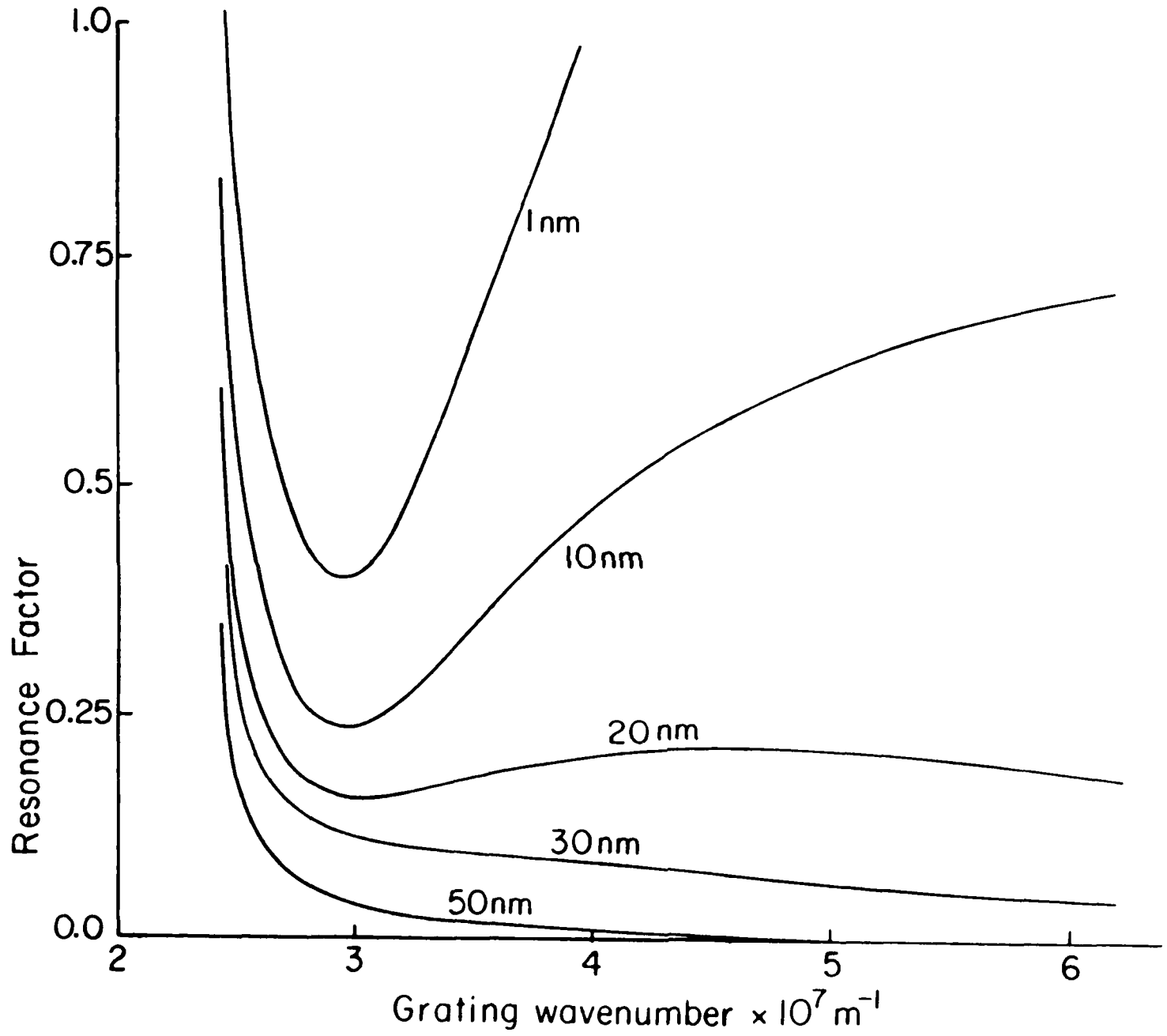
1.0
0.75
0.5
0.25
0.0
Resonance Factor
1nm
10nm
20nm
30nm
50nm
2
3
4
5
6
Grating wavenumber × 10^7 m^-1

Fig 3

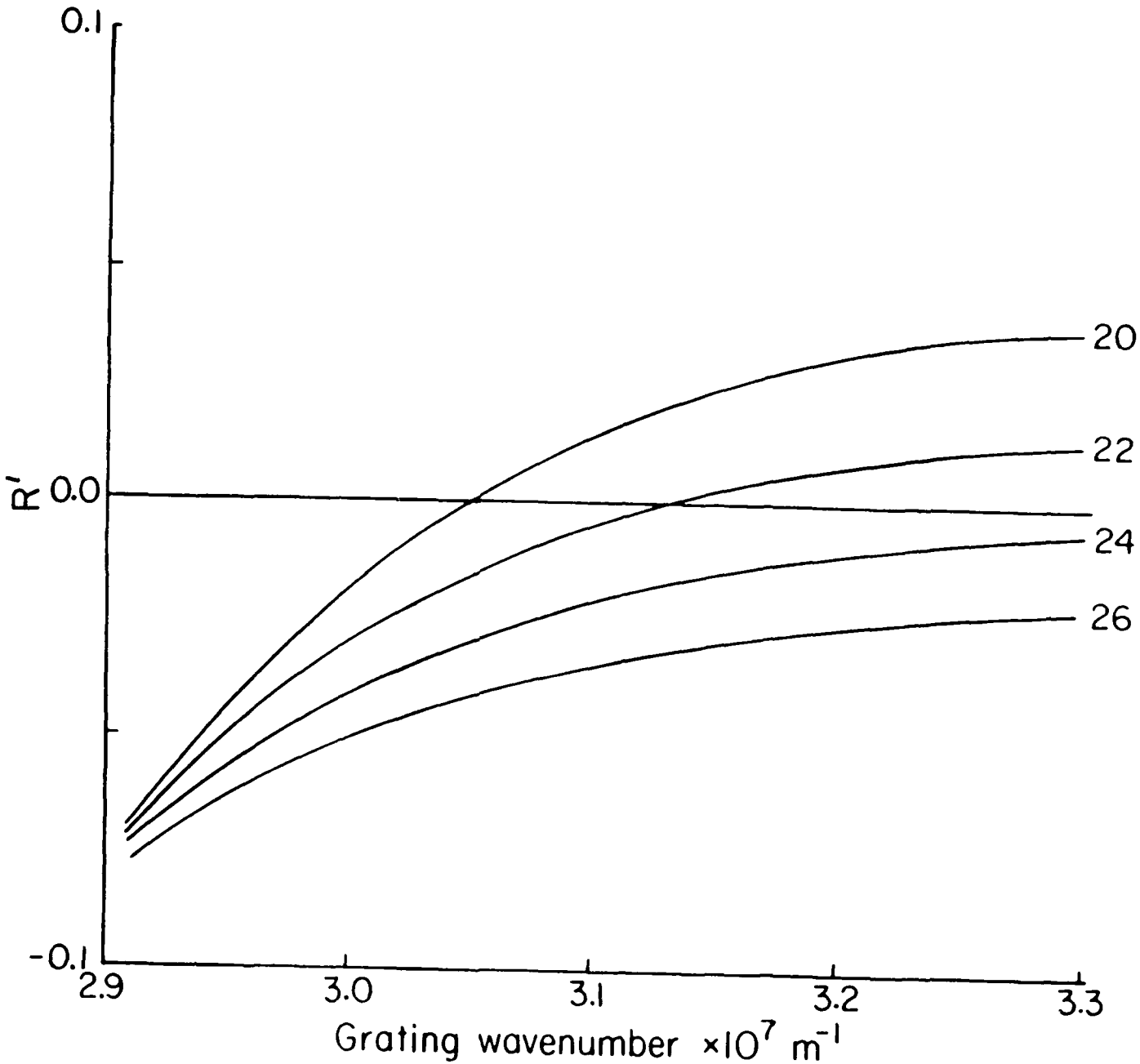
0.1
0.0
-0.1
$\tilde{R}$
20
22
24
26
2.9
3.0
3.1
3.2
3.3
Grating wavenumber $\times 10^7$ m^{-1}

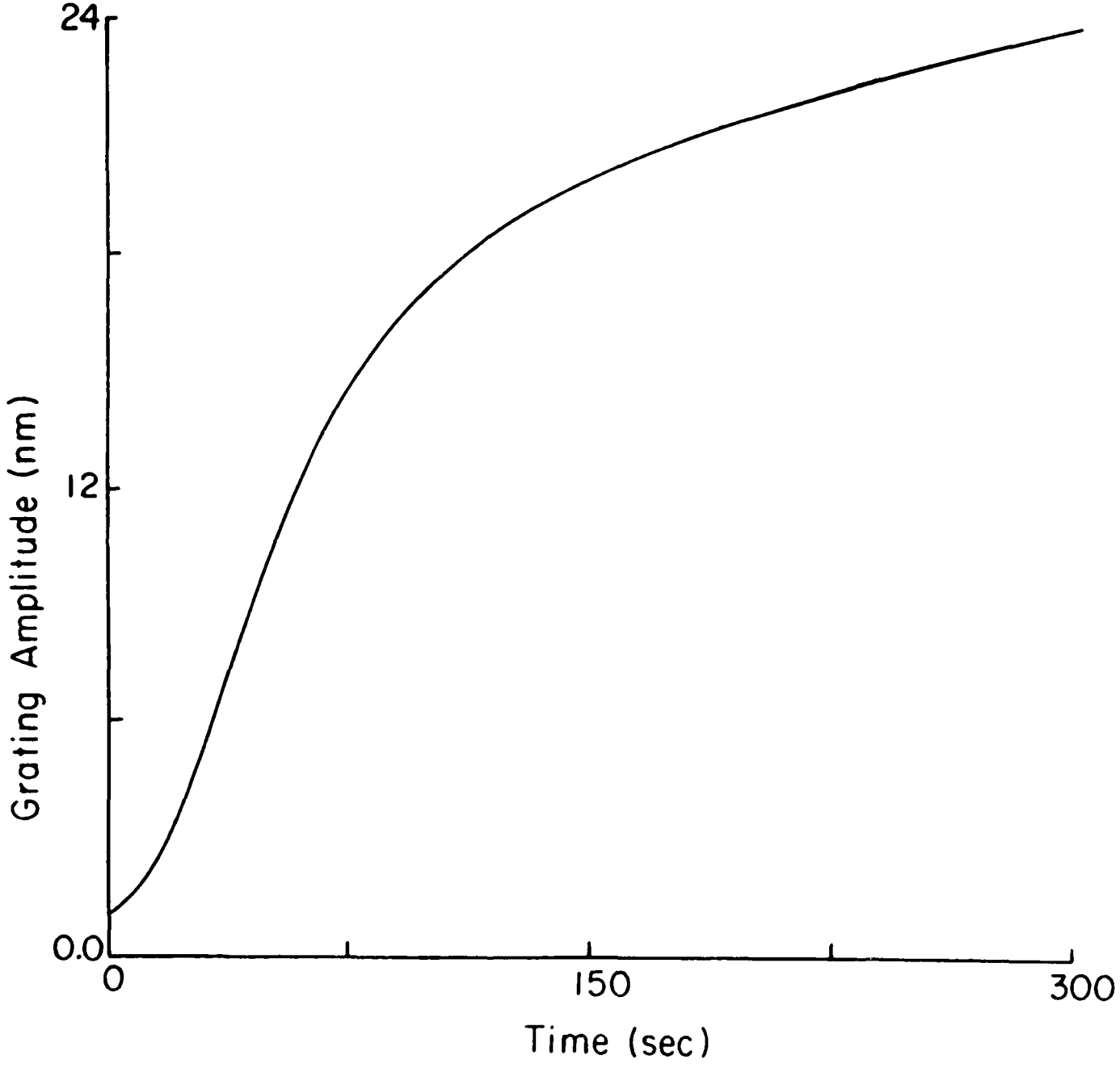

Fig 2a

TECHNICAL REPORT DISTRIBUTION LIST, GEN

	No. Copies
Office of Naval Research Attn: Code 1113 800 N. Quincy Street Arlington, Virginia 22217-5000	2
Dr. Bernard Douda Naval Weapons Support Center Code 50C Crane, Indiana 47522-5050	1
Naval Civil Engineering Laboratory Attn: Dr. R. W. Drisko, Code L52 Port Hueneme, California 93401	1
Defense Technical Information Center Building 5, Cameron Station Alexandria, Virginia 22314	12 high quality
DTNSRDC Attn: Dr. H. Singerman Applied Chemistry Division Annapolis, Maryland 21401	1
Dr. William Tolles Superintendent Chemistry Division, Code 6100 Naval Research Laboratory Washington, D.C. 20375-5000	1
Dr. David Young Code 334 NORDA NSTL, Mississippi 39529	1
Naval Weapons Center Attn: Dr. Ron Atkins Chemistry Division China Lake, California 93555	1
Scientific Advisor Commandant of the Marine Corps Code RD-1 Washington, D.C. 20380	1
U.S. Army Research Office Attn: CRD-AA-IP P.O. Box 12211 Research Triangle Park, NC 27709	1
Mr. John Boyle Materials Branch Naval Ship Engineering Center Philadelphia, Pennsylvania 19112	1
Naval Ocean Systems Center Attn: Dr. S. Yamamoto Marine Sciences Division San Diego, California 91232	1
Dr. David L. Nelson Chemistry Division Office of Naval Research 800 North Quincy Street Arlington, Virginia 22217	1

ABSTRACTS DISTRIBUTION LIST, 056/625/629

Dr. J. E. Jensen
Hughes Research Laboratory
3011 Malibu Canyon Road
Malibu, California 90265

Dr. J. H. Weaver
Department of Chemical Engineering
and Materials Science
University of Minnesota
Minneapolis, Minnesota 55455

Dr. A. Reisman
Microelectronics Center of North Carolina
Research Triangle Park, North Carolina
27709

Dr. M. Grunze
Laboratory for Surface Science and
Technology
University of Maine
Orono, Maine 04469

Dr. J. Butler
Naval Research Laboratory
Code 6115
Washington D.C. 20375-5000

Dr. L. Interante
Chemistry Department
Rensselaer Polytechnic Institute
Troy, New York 12181

Dr. Irvin Heard
Chemistry and Physics Department
Lincoln University
Lincoln University, Pennsylvania 19352

Dr. K.J. Klaubunde
Department of Chemistry
Kansas State University
Manhattan, Kansas 66506

Dr. C. B. Harris
Department of Chemistry
University of California
Berkeley, California 94720

Dr. F. Kutzler
Department of Chemistry
Box 5055
Tennessee Technological University
Cookesville, Tennessee 38501

Dr. D. DiLella
Chemistry Department
George Washington University
Washington D.C. 20052

Dr. R. Reeves
Chemistry Department
Renssaeler Polytechnic Institute
Troy, New York 12181

Dr. Steven M. George
Stanford University
Department of Chemistry
Stanford, CA 94305

Dr. Mark Johnson
Yale University
Department of Chemistry
New Haven, CT 06511-8118

Dr. W. Knauer
Hughes Research Laboratory
3011 Malibu Canyon Road
Malibu, California 90265

ABSTRACTS DISTRIBUTION LIST, 056/625/629

Dr. G. A. Somorjai
Department of Chemistry
University of California
Berkeley, California 94720

Dr. J. Murday
Naval Research Laboratory
Code 6170
Washington, D.C. 20375-5000

Dr. J. B. Hudson
Materials Division
Rensselaer Polytechnic Institute
Troy, New York 12181

Dr. Theodore E. Madey
Surface Chemistry Section
Department of Commerce
National Bureau of Standards
Washington, D.C. 20234

Dr. J. E. Demuth
IBM Corporation
Thomas J. Watson Research Center
P.O. Box 218
Yorktown Heights, New York 10598

Dr. M. G. Lagally
Department of Metallurgical
and Mining Engineering
University of Wisconsin
Madison, Wisconsin 53706

Dr. R. P. Van Duyne
Chemistry Department
Northwestern University
Evanston, Illinois 60637

Dr. J. M. White
Department of Chemistry
University of Texas
Austin, Texas 78712

Dr. D. E. Harrison
Department of Physics
Naval Postgraduate School
Monterey, California 93940

Dr. R. L. Park
Director, Center of Materials
Research
University of Maryland
College Park, Maryland 20742

Dr. W. T. Peria
Electrical Engineering Department
University of Minnesota
Minneapolis, Minnesota 55455

Dr. Keith H. Johnson
Department of Metallurgy and
Materials Science
Massachusetts Institute of Technology
Cambridge, Massachusetts 02139

Dr. S. Sibener
Department of Chemistry
James Franck Institute
5640 Ellis Avenue
Chicago, Illinois 60637

Dr. Arnold Green
Quantum Surface Dynamics Branch
Code 3817
Naval Weapons Center
China Lake, California 93555

Dr. A. Wold
Department of Chemistry
Brown University
Providence, Rhode Island 02912

Dr. S. L. Bernasek
Department of Chemistry
Princeton University
Princeton, New Jersey 08544

Dr. W. Kohn
Department of Physics
University of California, San Diego
La Jolla, California 92037

ABSTRACTS DISTRIBUTION LIST, 056/625/629

Dr. F. Carter
Code 6170
Naval Research Laboratory
Washington, D.C. 20375-5000

Dr. Richard Colton
Code 6170
Naval Research Laboratory
Washington, D.C. 20375-5000

Dr. Dan Pierce
National Bureau of Standards
Optical Physics Division
Washington, D.C. 20234

Dr. R. Stanley Williams
Department of Chemistry
University of California
Los Angeles, California 90024

Dr. R. P. Messmer
Materials Characterization Lab.
General Electric Company
Schenectady, New York 22217

Dr. Robert Gomer
Department of Chemistry
James Franck Institute
5640 Ellis Avenue
Chicago, Illinois 60637

Dr. Ronald Lee
R301
Naval Surface Weapons Center
White Oak
Silver Spring, Maryland 20910

Dr. Paul Schoen
Code 6190
Naval Research Laboratory
Washington, D.C. 20375-5000

Dr. John T. Yates
Department of Chemistry
University of Pittsburgh
Pittsburgh, Pennsylvania 15260

Dr. Richard Greene
Code 5230
Naval Research Laboratory
Washington, D.C. 20375-5000

Dr. L. Kesmodel
Department of Physics
Indiana University
Bloomington, Indiana 47403

Dr. K. C. Janda
University of Pittsburg
Chemistry Building
Pittsburg, PA 15260

Dr. E. A. Irene
Department of Chemistry
University of North Carolina
Chapel Hill, North Carolina 27514

Dr. Adam Heller
Bell Laboratories
Murray Hill, New Jersey 07974

Dr. Martin Fleischmann
Department of Chemistry
University of Southampton
Southampton 509 5NH
UNITED KINGDOM

Dr. H. Tachikawa
Chemistry Department
Jackson State University
Jackson, Mississippi 39217

Dr. John W. Wilkins
Cornell University
Laboratory of Atomic and
Solid State Physics
Ithaca, New York 14853

ABSTRACTS DISTRIBUTION LIST, 056/625/629

Dr. R. G. Wallis
Department of Physics
University of California
Irvine, California 92664

Dr. D. Ramaker
Chemistry Department
George Washington University
Washington, D.C. 20052

Dr. J. C. Hemminger
Chemistry Department
University of California
Irvine, California 92717

Dr. T. F. George
Chemistry Department
University of Rochester
Rochester, New York 14627

Dr. G. Rubloff
IBM
Thomas J. Watson Research Center
P.O. Box 218
Yorktown Heights, New York 10598

Dr. Horia Metiu
Chemistry Department
University of California
Santa Barbara, California 93106

Dr. W. Goddard
Department of Chemistry and Chemical
Engineering
California Institute of Technology
Pasadena, California 91125

Dr. P. Hansma
Department of Physics
University of California
Santa Barbara, California 93106

Dr. J. Baldeschwieler
Department of Chemistry and
Chemical Engineering
California Institute of Technology
Pasadena, California 91125

Dr. J. T. Keiser
Department of Chemistry
University of Richmond
Richmond, Virginia 23173

Dr. R. W. Plummer
Department of Physics
University of Pennsylvania
Philadelphia, Pennsylvania 19104

Dr. E. Yeager
Department of Chemistry
Case Western Reserve University
Cleveland, Ohio 41106

Dr. N. Winograd
Department of Chemistry
Pennsylvania State University
University Park, Pennsylvania 16802

Dr. Roald Hoffmann
Department of Chemistry
Cornell University
Ithaca, New York 14853

Dr. A. Steckl
Department of Electrical and
Systems Engineering
Rensselaer Polytechnic Institute
Troy, NewYork 12181

Dr. G.H. Morrison
Department of Chemistry
Cornell University
Ithaca, New York 14853

END

DATE

FILMED

APRIL

1988

DTIC